National University of Science and Technology
POLITEHNICA Bucharest
Doctoral school of Electrical Enginnering

SUMMARY DOCTORAL THESIS

INTELLIGENT SORTING SYSTEM OF LI-ION BATTERIES FROM THE AUTOMOTIVE INDUSTRY THAT HAVE REACHED THEIR END OF LIFE

Scientific coordinator:
Prof. PhD. Eng. George-Călin SERIȚAN

PhD student:
Eng. Iulian-Teodor VOICILĂ

Bucharest 2025

Acknowledgement

I take this opportunity to express in words what I may not have successfully conveyed verbally or through actions. I wish to extend my sincere thanks and appreciation to Prof. PhD. Eng. George-Călin Serițan for all the support and guidance provided throughout the completion of my doctoral thesis. Without your dedication and patience, I would not have been able to complete this ambitious project. You have always been there to guide and encourage me, offering valuable advice and support. Your knowledge and expertise have been fundamental to my academic and professional development. I am deeply grateful for the time and effort you have invested in my training and in the success of this work. I conclude these lines with the hope that I will, in turn, be able to carry forward the values and knowledge acquired under your careful guidance.

I also thank my colleagues, Conf. PhD. Eng. Bogdan-Adrian Enache and S. l. PhD. Eng. Irina Vîlciu, for the knowledge, wisdom, and moral support they generously provided in navigating the academic and emotional challenges necessary for this endeavor.

I thank my parents and friends who have been with me on this interesting journey. The discussions and mutual support were essential in undertaking this professional adventure. Sincere thanks for the patience and understanding they have offered me.

Last but not least, I want to thank my wife, who has been my pillar of support during difficult moments of doubt or uncertainty, helping me find myself, stay motivated, and, most importantly, keep my confidence. Without her love, encouragement, and support, it would have been hard for me to persevere.

I am deeply grateful to all of you for the support you have provided!

„My belief is firm in a law of compensation. The true rewards are ever in proportion to the labor and sacrifices made.” –

Nikola Tesla

CONTENT

Key words: sorting system, screening method, Li-Ion, Cascaded Buck-Boost, State of Health (SOH);

I. INTRODUCTION

Currently, climate change is the most significant concern for both industry and academia in the pursuit of sustainable development. One of the most challenging global objectives aimed at mitigating climate change is achieving carbon neutrality, a level of carbon emissions low enough to be safely absorbed by the planet's natural system [1]. One cause of the increase in carbon emissions is the automobile industry [2]. In 2014, globally, gasoline and diesel vehicles contributed 14% of carbon emissions (Environmental Protection Agency), while in the EU, this number reached 25% in 2018 [3]. Thus, one of the explored solutions is the replacement of current vehicles with electric ones. Consequently, there has been a substantial increase in the number of Electric Vehicles (EV) and Hybrid Electric Vehicles (HEV and PHEV). By 2050, various organizations predict that electric vehicles will constitute approximately 60% of the total car market [4]. Due to physical and chemical changes during their use, their batteries are retired within a time frame of less than 7 to 12 years, leading to the conclusion that, in the coming years, the batteries equipping this first generation of electric vehnicles and hybrid electric vehicles will reach their end of life (EOL), marking the point that triggers the process of their replacement [5], [6], [7], [8].

In Figure I-1, the stages of the life cycle for batteries used in the automotive industry are presented. After the production phase is completed, the batteries are intended for the automotive industry. They can support the energy required for the electric traction of vehicles until they reach about 75%-80% of their initial capacity [6]. The fate of decommissioned bateries is regulated in the EU by Directive 2000/53/EC – *A review of methods for analyzing dynamic material flows* and Directive 2006/66/EC – *Primary and Secondary batteries and waste*, which requires that battery manufacturers and local administrations have a complex system capable of properly collecting and recycling batteries when they are no longer functional [7]. Traditionally, after batteries have reached the end of life in their first phase of use, they end up in one of two cases:

1. Dismantling the battery pack and checking those that have not reached their end of life with the aim of reusing them by remanufacturing in the application for which they were designed (automotive industry);

2. Battery recycling for the extraction of secondary raw materials (Li, Ni, Co, etc.) in order to produce new batteries.

Battery recycling is an expensive process with a high degree of pollution, and the increased production costs are considered one of the major obstacles preventing the large-scale adoption of electric vehicles [7]. In this context, the second use of batteries is one of the solutions explored to reduce costs and pollution [9]. The concept of giving a second life to decommissioned batteries

simply involves reusing those that no longer meet the requirements of automotive industry but could still be used for less demanding applications, such as backup power supplies (UPS), household appliances, personal devices, small traction equipment, and other low-power drives [3], [10], [11].

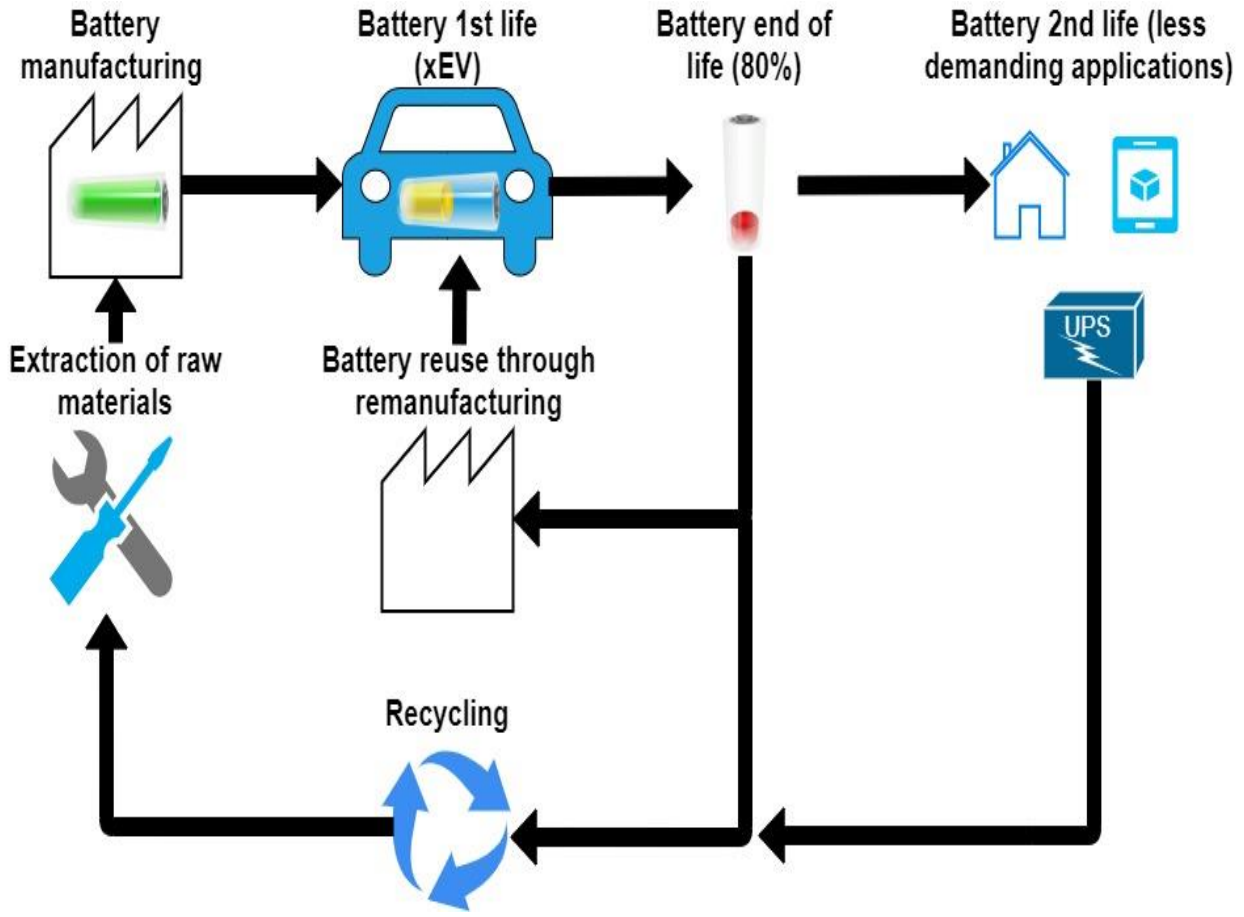

Fig. I-1. Schematic representation of life cycle stahes for batteries used in automotive industry.

These batteries are considered to be in their final phase of operation, but they still have approximately 80% of their nominal capacity. They are retired due to the automotive industry's safety regulations and transportation laws. This reuse concept will help extend the service life of batteries, reduce costs over their entire life cycle, and also popularize and generalize electric vehicles in the market [12]. Of course, the lifespan of batteries intended for reuse clearly depends on the energy requirements of the application, as explained in [13].

Thus, the process of reintegrating batteries retired from the automotive industry is presented below. Unlike the evaluation required before launching the battery on the market during its first use, the testing process for the second life is less demanding because destructive tests that evaluate thermal stress, overcharge response, over-discharge response, etc., are eliminated [14]. Therfore, the safety of these batteries is already proven before they are used in vehicles, and only the

evaluation to guarantee performance for the entire duration of the new life is necessary. However, before the actual evaluation of the batteries, they must undergo a preparation phase that includes the usage history and the reason why they can no longer be used in the automotive industry (physical damage, safety reasons, etc.) [15]. Once this information is collected, it can be decided whether the batteries are subjected to further performance tests; otherwise, they are removed from the process. If the first step is fulfilled, the next phase involves dismantling the modules down to the cell level, followed by performance evaluation [16]. Figure I-2 shows the process of reintegrating batteries into their second life cycle.

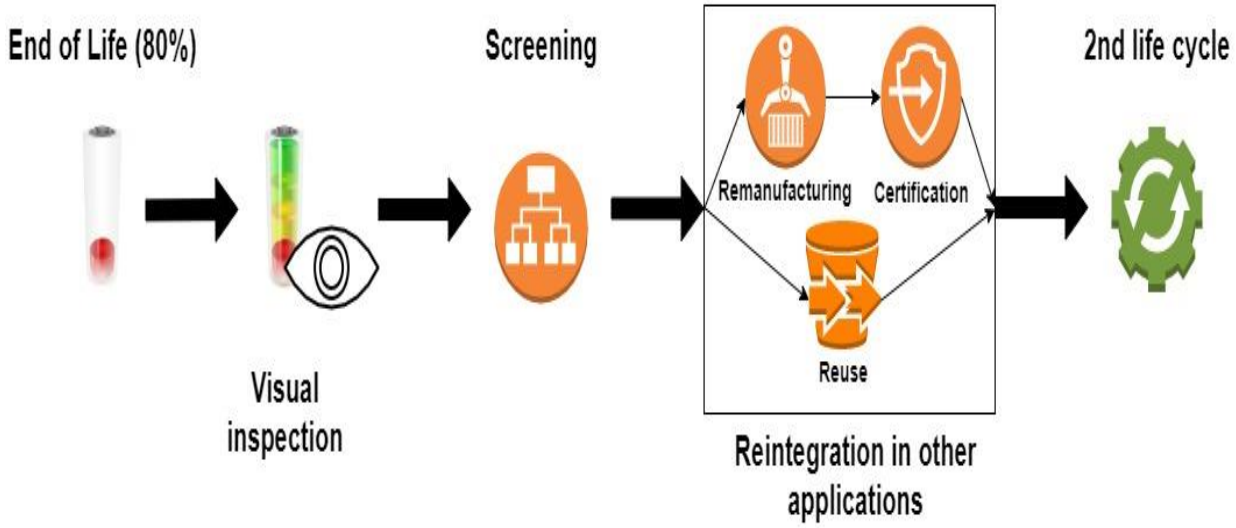

Fig. I-2. The reintegration process of batteries withdrawn from use in the second cycle of operation.

This process consists of two stages, in the first one all batteries are visually inspected to determine any obvious physical damage. The visual inspection initiates the process by eliminating batteries with potential defects such as corrosion, swelling, and material leakage [17]. Therefore, only batteries that pass the first test can be evaluated in the second stage, where they will be subjected to sorting methods. This stage assesses the state of health (SOH) and classifies the batteries according to certain criteria that depend on the battery chemistry and the energy application's requirements [15].

I.1 Problem formulation

The significant increase in the number of electric vehicles and hybrid electric vehnicles leads to the decommissioning of a very large number of batteries from the automotive industry. This raises the issue of environmental pollution and, consequently, human health, as the batteries equipping these vehicles will reach their end of life. Battery recycling is a traditional solution for manufacturing new batteries, leading to an increase in circularity and a reduction in the extraction

of new materials. On the other hand, these so-called end-of-life batteries still have approximately 80% of their initial capacity, which opens up new opportunities for their reuse in other applications with lower energy requirements than those in the automotive industry.

Integrating batteries into auxiliary applications requires a sorting process to evaluate their performance. This process occurs in two stages, the first stage involves a visual inspection to detect physical damage, while the second stage assesses the state of health (SOH) and classifies the remaining batteries for different energy applications. The core idea behind the second-life concept in the battery field is to properly evaluate the parameters to ensure that the new battery packs are as homogeneous as possible. Traditional approaches to sorting automotive batteries require lengthy testing times, are expensive, and serve to only one battery model. Moreover, the reduced flexibility for users to adapt the internal references of testing systems significantly diminishes interest from both the industry and customers.

The aim of this doctoral thesis is to develop a method and an automatic sorting system for Li-Ion batteries from the automotive industry that have reached their end of life, with the goal of reusing them in other applications. The proposed method for determining the state of health of the batteries is based on an intermediate presorting stage to reduce testing time, followed by the actual screening phase using a well-known method from the literature that offers high accuracy. Additionally, a system is proposed that uses a four quadrant bidirectional power converter, allowing simultaneous testing of two or more multi-technology cells.

The method and automatic sorting system will provide cost-effective, efficient, and rapid solutions for classifying reusable batteries according to their actual age, as well as ensuring a scalable and modular device for testing multiple cells simultaneously or extending the scope for testing modules or even battery packs. The operation of the automatic system based on the new algorithm comprises the following stages:

1. Selection of the battery type: LFP, LiPo, NMC etc.

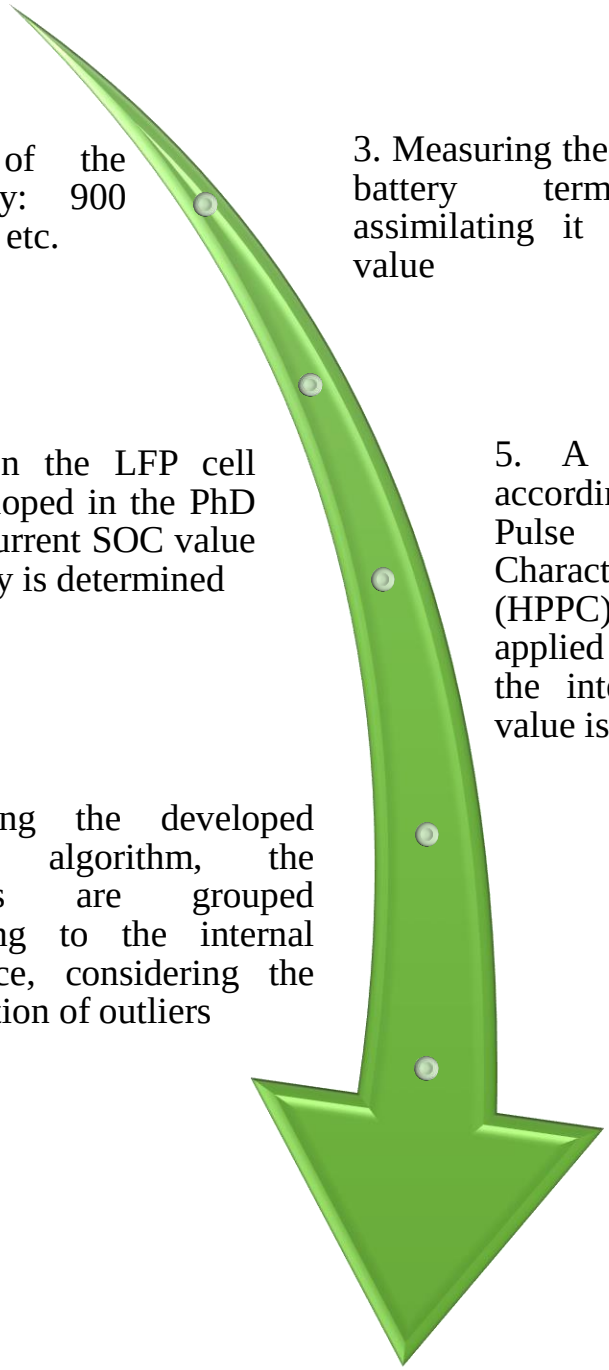

2. Selection of the battery capacity: 900 mAh, 1100 mAh etc.

3. Measuring the voltage at the battery terminals and assimilating it to the OCV value

4. Based on the LFP cell model developed in the PhD thesis, the current SOC value of the battery is determined

5. A test sequence according to the Hybrid Pulse Power Characterization Test (HPPC) profile is applied to this SOC and the internal resistance value is determined

6. Using the developed sorting algorithm, the batteries are grouped according to the internal resistance, considering the elimination of outliers

7. The approximate SOH of a single battery that characterizes the entire group is determined

I.2 Research objectives

The main objective of the doctoral thesis is the *development of system and an innovative method for fast and high-precision sorting* of Li-Ion batteries that have reached their end of life.

The secondary objectives of the PhD thesis are as follows:

Documentation

- Thorough documentation of the current state of methods for sorting retired batteries, aiming to develop and implement an innovative method.
- Detailed documentation of bidirectional DC-DC power converters topologies for designing and implementing the testing system for multi-technology batteries.

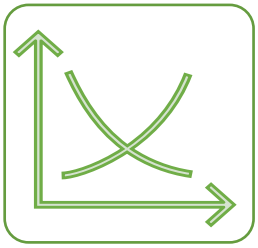

Design

- Design, modeling, and simulating the system in specialized software to study the behavior of analog and digital circuits, as well as batteries.
- Developing the code for controlling the power converter in accordance with the specific profiles from PNGV and USABC manuals.
- Developing the model to determine the relationship between SOC and OCV of the battery.
- Developing a model to determine the OCV of the battery with high accuracy.

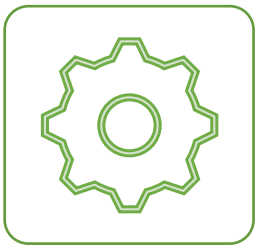

Validation

- Development of the battery sorting system prototype.
- Implementation and verification of the battery sorting system prototype.

In the research paper tilted „Intelligent sorting system of Li-Ion batteries from the automotive industry that have reached their end of life," I aimed to develop an innovative method for sorting retired batteries, significantly reducing the overall testing time. Additionally, the paper presents and proposes a sorting system capable of simultaneously testing 2N batteries of identical or different technologies. The sorting system is also designed to be modular and scalable.

I.3 Structure and contend of the thesis

The paper is structured into seven chapters that include the following:

In *Chapter 1 – Introduction* general aspects of battery sorting process are presented. It also outlines the problem formulation and how this paper aims to address it by establishing specific objectives.

Chapter 2 – Current status of sorting methods for retired batteries from the automotive industry is dedicated to studying the sorting methods for decommissioned automotive batteries. The chapter concludes with a comparative analysis based on four comparsion criteria to highlight the sorting methods with the most optimal characteristics.

In *Chapter 3 – Analysis of DC-DC power converters topologies used in battery sorting systems* a multi-criteria analysis of bidirectional DC-DC power converters is conducted to choose the optimal topology for testing multi-technology batteries.

Chapter 4 – Contributions to the development of the battery sorting method describes the implementation and functionality of the proposed battery sorting method, as well as the modeling of the algorithm for determining OCV and SOC.

Chapter 5 – Contributions to the structure of the sorting system includes the design and implementation of the system, from both hardware and software perspectives, and the study of the system's behavior through simulations in specialized programs (LTspice, Matlab/Simulink).

In *Chapter 6 – Development of source code for battery sorting* sequences of code used for power converter control, user interface creation, and sorting method implementation are highlighted.

În *Chapter 7 – Results and conclusions* the conclusions of the scientific activity conducted during the preparation of the doctoral thesis are presented, along with a reference to a series of future research directions.

I.4 Dissemination of results

The dissemination of results was achieved by publishing five scientific articles, of which two were as the first author and three as a co-author, in collaboration with the supervisory committee and other researchers. Additionally, a patent application was submitted to the State Office for Inventions and Trademarks (OSIM) titled "Method and System for Automatic Sorting of Batteries that Have Reached Their End of Life for Reuse." As part of the dissemination activities for the project results, besides the already published articles, two more scientific articles are currently in the process of being published, where I am the first author. The first paper, ***Voicila, T. I.***, *Seritan, G. C., Enache, B. A. (2024), Analysis of bidirectional DC-DC power converters for screening systems of retired batteries,,trimisă către Revue roumaine des sciences techniques, Serie Electrotechnique et Energetique - IF 0.7 WOS*, addresses the study of DC-DC power converters used in battery sorting systems as described in Chapter 2, where a multi-criteria analysis was performed to choose the optimal topology and validate its performance in the LTspice program.

The second paper, ***Voicila, T. I,*** *Enache, B. A., Argyriou, V., Sarigiannidis, P., Seritan, G. C. (2024), Enhanced OCV estimation in LiFePO4 batteries: A novel statistical approach leveraging real-time knee/elbow detection,* submitted to the *Journal Engineering, Technology & Applied Science Research (ETASR) – IF 1.5 WOS,* discusses the dependency between the state of charge (SOC) and the open-circuit voltage (OCV) of batteries to reduce estimation errors, a topic covered in Chapter 4.

In the first part of the research, I studied Sheperd's equations for battery modeling in Matlab/Simulink because they require a limited number of parameters. These can be obtained from the battery manufacturer's data or based on an experimental data set. Moreover, these equations are already part of the battery model found in the program, and thus the proposed algorithm can be extended to any technology by introducing the coordinates of the marked points from the nominal discharge characteristic. The study was conducted for a Pb-Acid battery, with data extracted from the manufacturer's datasheet, in the paper: *Gandescu, C. H., Gkanatsios, S., Cepisca, C., Vilciu, I., &* ***Voicila, T. I.*** *(2022). Accurate Modelling of an Online Uninterrupted Power Supply. Journal of Electrical Engineering, Electronics, Control and Computer Science, 8(4), 45-50*. The model was further extended for a LiFePO4 battery and used in a system for sorting retired batteries in the paper: ***Voicilă, T. I.****, Seriţan, G. C., Enache, B. A., Stănculescu, M., & Porumb, R. (2023), Design and implementation of a multi-battery, multi-chemistry state of health screening system. In MPS Cluj 21-23*. The proposed system includes a cascaded bidirectional Buck-Boost power converter that allows simultaneous testing of two or more batteries. In this paper, the internal resistance of the batteries was determined to evaluate their state of health. Based on the results obtained in previous research, we aimed to continue verifying the proposed sorting system. The aforementioned paper focused on studying the behavior of LFP batteries, modeled with real experimental data, but the operation of the power converter was not sufficiently analyzed. Therefore, for the analysis of the electronic circuit, the proposed system was implemented in the LTspice simulation program. The schematic used macromodels of the LTC4444 control circuit, as well as power switches, capacitors, inductors, snubber, etc. The research culminated in the publication of the paper: ***Voicilă, T. I.****, Seriţan, G. C., Enache, B. A., Porumb, R., & Stănculescu, M. (2023). First Steps Towards the Design of a multi-Chemistry, multi-Battery State of Health Screening System. In 2023 13th International Symposium on Advanced Topics in Electrical Engineering (ATEE) (pp. 1-6). IEEE*. To determine the state of health of Pb-Acid batteries, the two-pulse discharge method at constant current was used, which resulted in errors of less than 5%. The study was materialized in the paper: *Gkanatsios, S., Vilciu, I., &* ***Voicila, T. I.*** *(2023). Evaluating the state of health of Lead-Acid battery used in UPS. EMERG: Energy. Environment. Efficiency. Resources. Globalization, 9(3)*. Another subject of interest was the loss of capacity when batteries are unused for an extended period. The study resulted in the publication of the paper: *Constantinescu, L. M., Enache, B. A., Dogaru, V. G.,* ***Voicila, T. I.****, Vilciu, I., & Vasile, S. C. (2023). Statistical Analysis of Capacity Loss for Stored Batteries. In 2023 15th International Conference on Electronics, Computers and Artificial Intelligence (ECAI) (pp. 01-04). IEEE*.

Derived from the main research direction, other secondary objectives were achieved, resulting in four research papers aimed at improving the teaching process, including: *Grigorescu, S. D., Seritan, G. C., Enache, B. A., Adochiei, F. C., Argatu, F. C., Vilciu, I., &* ***Voicila, T. I.*** *(2022). A Multipurpose Video Immersion Laboratory. In 2022 E-Health and Bioengineering Conference (EHB) (pp. 1-4). IEEE.*; studying air quality in the paper: *Vîlciu, I., Enache, B. A., Seriţan, G. C., &* ***Voicilă, T. I.*** *(2023). An Indoor Air Quality Score Computation and System. In 2023 13th International Symposium on Advanced Topics in Electrical Engineering (ATEE) (pp. 1-4). IEEE.*; and integrating smart devices in the medical field in the papers: ***VOICILA, T. I.****, BOGDAN, A.-G., ENACHE, B.-A. (2023). Guidelines for developing an IOT-enabled application for enhanced hospital management, University of Pitesti Scientific Bulletin Series: Electronics and Computer Science, 23(2), pp. 1-6* and ***VOICILA, T. I.****, BOGDAN, A.-G., ENACHE, B.-A. (2023). Comparative analysis of medical equipment identification techniques: A multifaceted approach for enhanced hospital operations, University of Pitesti Scientific Bulletin Series: Electronics and Computer Science, 23(2), pp. 7-12*.

II. Current status of sorting methods for retired batteries from the automotive industry

Various battery sorting methods have been proposed over the years and these can be classified into three categories: sorting methods based on complete charge-discharge cycles, methods based on battery parameters (OCV, SOC, Rin, etc.), and hybrid sorting methods based on intelligent algorithms, statistical analysis, and adaptive approches. Figure II-1 presents the classification of these methods according to the principle used. For methods based on complete charge-discharge cycles, we find constant current (CC) profiles, constant voltage (CV) profiles, and constant current followed by constant voltage (CCCV) profiles. Methods that utilize specific battery parameters include: current integration over time (Coulomb Counting), open circuit voltage measurement (OCV), impedance determination, internal resistance determination, incremental capacity analysis (ICV), differential voltage analysis (DVA), etc. Hybrid methods generally employ intelligent algorithms (Fuzzy Logic, Neural Networks, etc.) in combination with other methods to optimize the process.

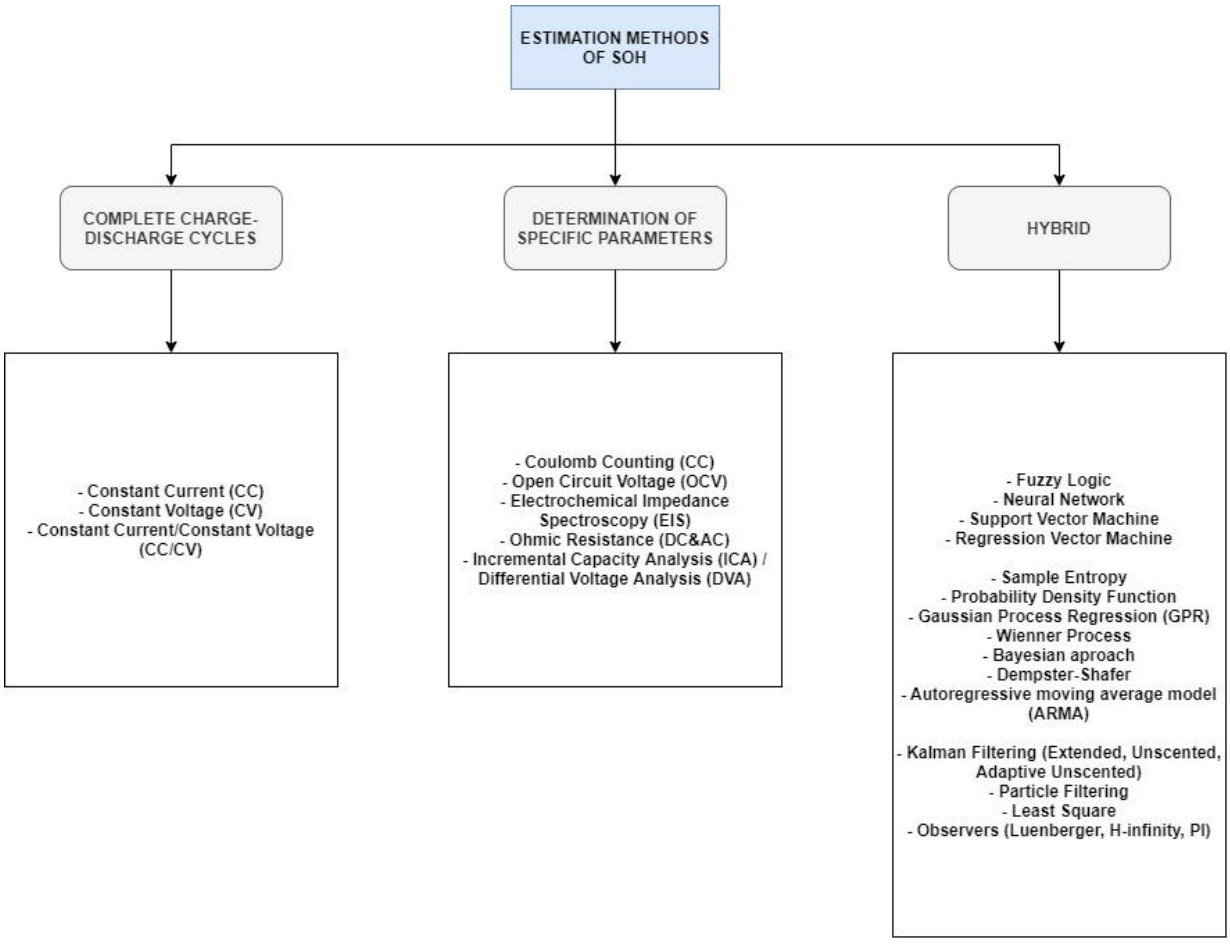

Figura. II-1. Classification of methods for determining the state of health (SOH) [3], [18], [19].

The SOH of a battery evaluates its condition and current performance level compared to its initial state. This parameter cannot be directly calculated like voltage or current, and it lacks a clear definition, making it difficult to analyze. To estimate battery performance, literature suggests using parameters related to SOH, such as capacity, impedance, internal resistance, state of charge, open circuit voltage, etc. To quantify this parameter, the following two equations are defined [20], [21]:

$$SOH = \frac{C_{now}}{C_{initial}} \cdot 100\ [\%] \tag{1}$$

$$SOH = \frac{R_{EOL} - R_{now}}{R_{EOL} - R_{initial}} \cdot 100\ [\%] \tag{2}$$

where $C_{initial}$ represents the battery's capacity when it exits the manufacturing process, C_{now} represents the battery's capacity at a given time after usage, $R_{initial}$ represents the battery's internal resistance when it exists the manufacturing process, R_{EOL} represents the battery's internal resistance at the end of its first use, and R_{now} represents the battery's internal resistance at a given time after usage.

II.1 Preliminary conditions regarding battery sorting

The evaluation of the battery, regardless of the application in which it will be integrated in its second life, is absolutely necessary to determine its current performance. This evaluation is important because the lifespan of the batteries inteded for reuse is unknown. It depends on how they were used in the first life cycle and how they will be used in the future [22]. Various factors related to the aging mechanism necessitate preliminary sorting processes to identify batteries with suitable characteristics. Otherwise, batteries with poor consistency can be easily overcharged or overdischarged, leading to excessive heating, explosions, internal short circuits, etc. [15]. Such a study allows for the proper characterization of cells in terms of specific parameters to ensure the selection is as homogeneous as possible [23]. Given the diversity of battery models on the market, it is useful to know the basic elements and performance criteria that define them to make meaningful comparisons. Any battery is characterized by a series of technical parameters, some of which are commonly provided by the manufacturer in the specification catalog, while the rest are defined through measurements taken in the laboratory or during use. These parameters explain the correct way to use the battery to achieve the highest efficiency.

II.2 Sorting methods based on complete charge-discharge cycles

Sorting methods based on charge-discharge cycles involve subjecting the battery to a partial or complete cycle of charging at a current or voltage specified by the manufacturer. After a

relaxation period, the battery undergoes a discharge cycle at the nominal current until the cut-off voltage is reached. A partial cycle refers to charging the battery at a *constant current* (CC) or at a *constant voltage* (CV), while a complete cycle represents the *constant current - constant voltage* (CCCV) charging profile.

II.3 Sorting methods based on determination of specific parameters

The *Coulomb Counting* method is one of the most widespread methods for determining the state of health (SOH) of batteries, regardless of their chemistry [24]. This method involves measuring the effective capacity using the charge-discharge process and determining the SOH using equation (1). The method involves two stages: in the first stage, the battery's effective discharge capacity is determined, correlated with a 0% state of charge by integrating the current over time, and in the second stage, the SOH is calculated. The *OCV* method for determining the battery's state of health involves defining the dependency of SOH on the open-circuit voltage. As presented in [24], based on monitoring the open-circuit voltage, the SOC-OCV characteristic is constructed, which can be used for all types of batteries, with the note that it differs for each one. The method for determining *internal resistance in direct current* (DC) or *alternating current* (AC) can be performed in two ways. The first method refers to studying the battery's behavior in direct current, which involves discharging or charging the battery and measuring the resistance using Ohm's law, i.e., the ratio between the voltage difference before and after discharge and the discharge current. The method for determining internal resistance in AC involves injecting an alternating signal with a frequency of 1 kHz or higher to excite the battery. Then, Ohm's law is applied to calculate the resistance [25]. Thus, the electrical impedance is the ratio between the variation of the voltage and that of the current, and describes both the relative amplitude of the two parameters and the relative phase. As with the method of determining the internal resistance in AC, the *EIS (Electrochemical Impedance Spectroscopy)* method uses an alternating signal of small amplitude with frequencies between 0.025 Hz and 4 kHz [3]. After applying the signal, the internal impedance of the battery is determined by plotting the dependence between the imaginary and real parts using the Nyquist plot. Another widely applicable method for battery characterization by identifying the aging mechanism is *ICA/DVA (Incremental Capacity Analysis / Differential Voltage Analysis)* and is defined according to [26] as follows. IC is determined based on the difference in capacitance due to the change in battery terminal voltage, while DV analysis is defined as the inverse of IC. Peaks on the voltage charge/discharge curve represent phase transitions between electrodes, and peaks on the capacitance charge/discharge curve indicate phase points at equilibrium.

II.4 Hybrid sorting methods

Hybrid methods are obtained by using intelligent algorithms (NN – Neural Networks, FL – Fuzzy Logic, KF – Kalman Filter, SVM – Support Vector Machine, RVM – Relevance Vector Machine, etc.) together with one or more techniques mentioned previously, so that the sorting process to be fast and accurate [27]. The *Fuzzy Logic* method is based on Boolean logic and predefined categories or sets of conditions. A fuzzy function is applied to an input *x* that is part of a fuzzy set *A*, and the output is a number between 0 and 1 that represents the degree of membership of the input x to the set A. In fuzzy logic, the AND logical operators are used, OR and NOT [24]. When determining battery SOH, the output can be defined as a set of predefined responses, for example: unacceptable status, acceptable status, excellent status. The *Neural Networks* method is a mathematical model that tries to imitate the functioning of the human brain with the help of artificial neurons distributed on three levels: input neurons, output neurons and neurons that create connections between inputs and outputs. In the first level there is the purchased input data that serves to realize the second level. At this stage each neuron has a mathematical function implemented that determines a weighted result based on the inputs. The higher the weight, the better sensitivity is obtained [26]. The last layer predicts the output values and becomes more and more performant as the algorithm is trained for longer or the complexity is increased by the number of intermediate neurons. The *SVM (Support Vector Machine)* method is an algorithm that analyzes the input data and builds a model of the relationship between the input and output quantities. The degree of difficulty of the model increases in proportion to the amount of information used to train the algorithm [26]. *SampEn (Sample Entropy*) is a statistical method that analyzes the response of the voltage variation at the battery terminals in the aging process, thus being able to monitor the battery capacity [3]. Probabilistic methods are increasingly used in battery health determination systems. One of the most well-known is the *Probability Density Function (PDF)* which is defined as a function of continuous random variables within a certain interval. Another SOH estimation method that is increasingly widespread among probabilistic methods is the *Gaussian Process Regression (GPR)* method. The Gaussian process is defined as a set of random variables that characterize the probability distribution for each finite subset of variables, described by the mean of the values (μ) and covariance (Σ). A method widely used in the specialized literature is *Kalman Filtering (KF)*. Kalman Filtering is an adaptive method that analyzes the dynamics of the series of measurements and estimates the output variables based on them [28]. This method involves a two-step process. In the first stage, a prediction of the system states is made for which the output variables are determined. Then, in the second step, the estimated variables are updated so as to achieve the highest possible accuracy [29]. An alternative to the KF method is the *Particle Filter* (PF) method where the only difference between the two methods is given by the fact that PF does not assume a zero mean of the model states and noises for the Gaussian distribution [30]. The output response of the method is an estimate of the probability density function based on a set of weighted points (particles), which are values sampled from the state space with the highest relative probability.

From the analysis and description of the previously realized methods, it can be observed that the approaches of the methods fall into one of two categories:

- either they are fast methods with relatively low precision and low/medium complexity;
- either are methods that require historical data from the battery's operating period to improve results and thus involve longer testing time and increased complexity, but have very high accuracy.

II.5 Comparative study of battery sorting methods

Taking into account the previous analysis, a comparative study of the sorting methods was carried out which, as presented, is classified into three categories, namely: methods that use complete charge-discharge cycles (CC, CV, CCCV), methods that determine specific parameters (C, OCV, Rin) and hybrid methods (FL, NN, PF) that use smart algorithms and merge with other methods to increase performance. For each method within a group, a characterization was made according to complexity, state of health determination error, advantages and disadvantages. From the point of view of complexity, the methods are characterized on three levels, low, medium and high complexity. The error is expressed as a percentage, and the advantages and disadvantages are considered to highlight the computational effort, the widespread application of the method, and the possibility of improving the method. In Table II-1, the comparative study carried out for the battery sorting methods in order to determine the state of health is presented.

Tabel II-1. Comparative study of battery sorting methods for determining state of health

Methods		**Criteria**			
		Complexity	**Error**	**Advantages**	**Disadvantages**
Complete charge-discharge cycles [31], [32], [33], [34], [35], [36]	**CC**	Medium	2-5%	-Low power computation -Precise -Reliable	-It cannot be widely applied -Long operating time -Involves data processing to improve performance
	CV	Medium	<5%		
	CCCV	Medium	<3%		
Determination of specific parameters	**Coulomb Counting**	Low	1-10%	-Low power computation	-Increasing performance involves using a hybrid method

[3], [23], [24], [33], [37], [38], [39]				-Low power consumption -Easy to implement	-Requires recalibration on the test environment
	Open Circuit Voltage	Low	1-20%	-Fast -It can be easily implemented with other methods	-It cannot be widely applied -Requires time for OCV-SOH correlation
	Electrochemical Impedance Spectroscopy	Low	2-15%	-Avoids complicated calculations unless used in combination with other methods -High reliability	-It is used especially for batteries from the Li-Ion family -Requires dedicated equipment
	DC Ohmic Resistance	Low	<4%	-Fast -Precise -Requires low computing power	-It is sensitive to many factors -Can't be applied often
	AC Ohmic Resistance	Medium	<4%	-Fast -Quickly detect the existence of a defect	-The results obtained may differ depending on the frequency used -It is sensitive to many factors
	Incremental Capacity Analysis / Differential	Medium	1-3%	-It can be widely applied -Can be applied to any type of battery from the Li family	-Sensitive to noise and changing battery performance -Requires the application of filtering algorithms

	Voltage Analysis				
Hybrid [5], [29], [31], [36], [40], [41], [42], [43], [44], [45], [46], [47], [48], [49], [50]	**Fuzzy Logic**	High	1.4-10%	-It can be used for any type of battery -High adaptability	-Performance depends on the training process -Very high computational effort
	Neural Network	High	0.28-8%	-It can be used for any type of battery -Uses easy-to-measure parameters	-It needs a lot of data for training -Requires high-performance equipment
	Support Vector Machine (SVM)	High	<2%	-High accuracy -Low prediction time	-It is very complex -Accuracy depends on the quality of the measurements
	Sample Entropy	High	1.2%-2%	-It can be used for any family of batteries -Can be applied both offline and online	-It requires combining with other smart methods -High complexity
	Probability Density Function	Medium	2%	-Much better accuracy than curve fitting methods -Relatively easy to implement	-All studies apply the method to Li-Ion batteries -Requires battery tests beforehand
	Gaussian Process Regression	Medium	0.5%-3.5%	-Low implementation cost -High versatility	-Requires data processing beforehand -Sensitive to the chosen covariance function

	Kalman Filtering	Medium	0.5-8.3%	-It can be applied to any type of battery -High accuracy	-It requires storing a lot of data -Requires data processing
	Particle Filtering	High	0.4-12%	-It can be used for any family of batteries -High accuracy	-It requires a lot of data to train the model -Requires precision measurements

Based on the comparative study of sorting methods for batteries in the automotive industry, presented in Table II-1, it is observed that each method presents interesting characteristics, when the advantageous points are represented by accuracy and calculation speed. But, there is always a compromise, either the method is difficult to implement or the computational effort is too high.

Considering the increasing number of end-of-life batteries that will appear in the near future, I believe that the optics of sorting methods must change, and the focus will be on the development of very fast methods. As for the accuracy of the methods, it should be below 3%. This value represents the initial inconsistency of battery capacity from any battery with a BMS (Battery Management System). Although the retirement of the first generation of batteries equipping electric vehicles and hybrid electric vehicles due to the operating limit will happen soon, we must consider the end of life of the next generation because most batteries have a lifetime of 8- 12 years, and the need for energy is constantly increasing.

III. Analysis of DC-DC power converters topologies used in battery sorting systems

An important element of the test system is the DC-DC conversion structure used. This is responsible for the energy efficiency of the conversion and the flexibility of the system through the possibility of changing the current and voltage polarity. Considering that this paper proposes the power transfer between two multi-technology type batteries, one of the batteries will be discharged while the other battery will be charged, then the design and realization of a static current converter will be considered bidirectional continuous. In the following, a comparative study between the topologies of bidirectional DC-DC converters is presented. In order to determine the optimal topology, the most important characteristics of converters of this type were defined, and then a multicriteria analysis was applied. From the obtained results, the topology with the highest score will be chosen, for which the procedure will be continued in order to dimension and practically realize the chosen conversion structure.

Considering the large number of criteria and the variety of options for each criterion considered in the comparative analysis, a multicriteria analysis (MCA) will be used. This technique allows structuring and combining several criteria simultaneously in order to make a decision for a complex situation. So for each individual criterion a score between 0 and 100 will be assigned, where 100 means the most favorable case. After constructing the matrix with the allocation of scores, the performance matrix will be made in which each criterion receives a weight expressed as a percentage, so that their sum is equal to 100%. The weights are distributed and described as follows: the type of operation receives a weight of 15%, the number of coils and/or transformers 10%, the number of capacitors 10%, the number of switches 5%, the number of diodes 5%, the power density 15%, complexity 10%, size 10%, cost 5% and efficiency 15%. By summing the weights, a maximum of 100% is obtained. This weighting scheme aligns with the methodology established in [51].

Following the multi-criteria analysis, it was determined that the cascaded Buck-Boost topology represents the best solution among the studied topologies and will be further used in order to dimension, simulate the circuit and design the proposed solution.

IV. Contributions to the development of the battery sorting method

Once the batteries have reached their service limit, i.e. when the effective capacity is 80% of the rated capacity, they are withdrawn from use. According to the notions previously presented in relation to the reuse of batteries, it was discussed that they should be tested before being installed in other applications. To this end, the first step is to carry out a visual inspection, and then the actual testing. Batteries that do not meet the technical test norms are sent directly to recycling or are completely removed. To reduce the overall testing time this thesis proposes a new battery evaluation method. Thus, before the batteries are sorted using one of the methods mentioned earlier, an intermediate pre-sorting step is carried out whereby the batteries are grouped according to their internal resistance, so that only one battery is fully evaluated.

IV.1 Presentation of the innovative technological flow for battery sorting

Figure IV-1a shows the reintegration phases of batteries withdrawn from use in other applications with lower energy requirements than those in the automotive industry.

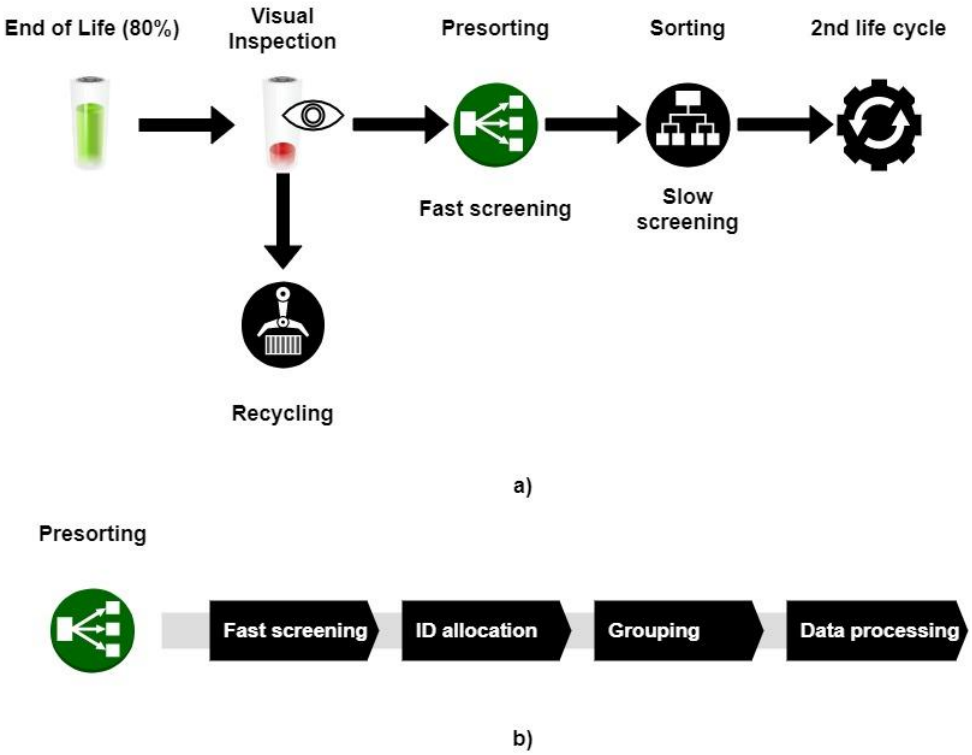

Figura. IV-1. The stages of the retired batteries sorting method.

In this presorting stage, a constant current pulse is applied: a charging pulse for the battery with the lowest state of charge (SOC) and a discharging pulse for the battery with a higher state of

charge (SOC). The duration of the pulse, as well as the amplitude of the signal, is set according to the USABC manual [52]. Thus, before applying the current pulse, the voltage at the battery terminals is measured to determine the open-circuit voltage (OCV). After the partial discharge/charge, the voltage at the battery terminals is measured again. Based on these voltages, and knowing the value of the imposed current, the internal resistance of the batteries can be determined using Ohm's law. Therefore, the internal resistance of the batteries will be equal to the ratio between the difference in voltage after the pulse application and the open-circuit voltage, and the value of the current pulse.

Figure IV-1b provides an extended description of the presorting stage. Initially, the internal resistance of the battery is determined according to the previously described procedure. Then, each battery is assigned an identifier that considers the battery's chemistry, its technical characteristics, and its serial number. After testing all the batteries, they are grouped based on internal resistance, and any batteries deviating by more than one standard deviation are eliminated from each group. Finally, the standard sorting procedure is resumed using a slow method to determine the state of health of the batteries. It is noteworthy that only one battery from a group is tested in detail, and this battery will characterize the entire group.

IV.2 Implementation of the presorting stage

Characterizing retired batteries is essential for creating a new battery pack with as similar characteristics as possible and ensuring proper functionality, regardless of the application in which it will be integrated. However, these electrochemical systems exhibit a high degree of complexity and are defined by nonlinear behavior, making their characterization challenging. The main parameters that characterize them are internal resistance and battery capacity [53], [54]. Accuracy, testing time, and necessary infrastructure are major barriers to reducing costs and optimizing techniques for evaluating battery state of health. Proper evaluation is a major criterion for maximizing lifespan, reducing safety issues, and ensuring economic and technical viability [55], [56], [57].

Regarding the value of impedance or internal resistance, it is difficult to assign a unique value due to its dynamic nature, which is susceptible to both internal factors (solid electrolyte interface layer, internal wiring resistance, current collector, hysteresis phenomenon) and external factors (temperature, state of charge, usage history, load) [56], [58]. Therefore, determining internal resistance is feasible only if accompanied by a detailed description of the conditions under which the measurement was performed [59].

The DC pulse method involves applying a current pulse and measuring the voltage response at the terminals after a well-defined duration, as shown in Figure IV-2. Thus, the open-circuit voltage (U_{OC}) is measured before applying the pulse, and the voltage (U) is measured after the application. Using Ohm's law, the internal resistance is determined. It is noteworthy that the

value of internal resistance depends on the amplitude of the current pulse, its duration, and the pulse profile, whether charging or discharging [60].

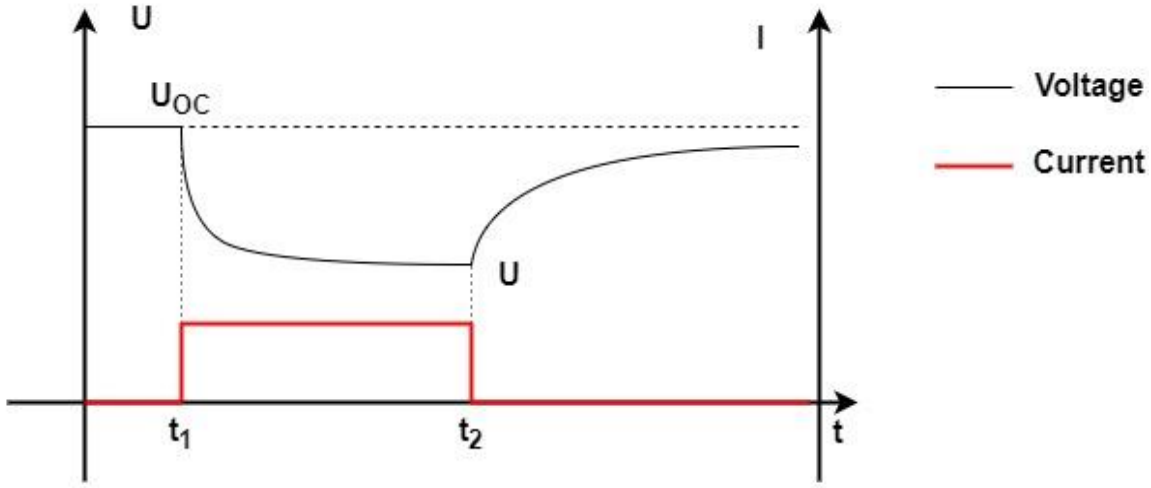

Figura. IV-2. Battery terminal voltage response to the application of a charging current pulse.

Internal resistance is inversely proportional to the applied current pulse and is affected by the hysteresis phenomenon. The voltage measured at the battery terminals will rise more quickly for a higher load due to the acceleration of the chemical process. As a result, the state of charge of the battery can change significantly enough to lead to an incorrect analysis of the current state of charge compared to the actual one [61]. Additionally, a too short duration will not be sufficient to capture all resistive elements [62]. According to various standards (ISO, EUCAR, USABC) and studies on the duration of the current pulse, it is generally shorter than 20 seconds [61].

.

IV.3 Presentation of the grouping stage

The method is based on the premise that the tested batteries have not been used for more than an hour, so the output voltage at the battery terminals can be regarded as the open circuit voltage (OCV). Thus, to determine the state of charge (SOC), a higher-order polynomial model is used to approximate this value based on the open circuit voltage (OCV). In this paper, a new method for determining OCV is proposed, which does not use a fixed rest period of 1 hour. Instead, the stopping criterion is based on the stabilization voltage variation when it falls within the range of ±1mV/hour or when the maximum duration of 24 hours is reached. Using this criterion ensures the stabilization of deeper electrochemical processes, ensuring an accurate measurement of the OCV. A similar stopping criterion is used in other works to evaluate the SOC-OCV relationship, with errors exceeding 7% for OCV estimation [63], [64], [65]. Notably, a hybrid method proposed in [66] involves an initial 24-hour testing period, followed by a secondary 5.2-hour test and a transition from a normal to a logarithmic time scale. This method achieves an OCV estimation

error of less than 1%. Based on this method, a new technique for evaluating the SOC-OCV relationship was developed. Instead of using two distinct points from the rest curve—one at 1 hour and another at the end of the 24-hour relaxation period—a new point corresponding to the knee/elbow point of the curve was introduced. This point signifies the transition from a region where the voltage varies significantly to one where it becomes more stable and linear, thus capturing the complex interaction of various electrochemical processes..

To develop the algorithm, a new 1.1 Ah LFP APR battery was used to determine the statistical model for estimating OCV. This battery was subjected to the USABC testing procedure to determine its effective capacity by using a constant discharge sequence with three different currents: C1/1, C2/2, and C3/3.

These data served as input parameters for the developed multivariable regression model. The model was divided into two separate sub-models to reduce estimation errors caused by the hysteresis phenomenon: one for estimating OCV after charging and one for estimating OCV after discharging. Once the hypotheses were verified, the multiple regression coefficients for each model were calculated and are presented in equations (3) and (4).

$$OCV_{charge} = -0.135 \cdot U_{initial} + 1.215 \cdot U_{elbow} - 0.272 \quad (3)$$

$$OCV_{discharge} = -0.112 \cdot U_{initial} + 1.063 \cdot U_{knee} + 0.162 \quad (4)$$

A preliminary evaluation of the proposed model was performed using statistical methods. Thus, the values of R and R^2 were calculated, resulting in values of 0.99 for R and 0.99 for R^2. These results indicate that the model has a high prediction accuracy of 99% and that 99% of the variation in the dependent variable is explained by the independent variables. Next, to evaluate the accuracy of the developed model, a battery testing procedure will be carried out for different SOC values, as well as for a new data set acquired from another 1.5 Ah LFP battery from a different manufacturer. SOC levels of 50% and 60% were specifically chosen due to the plateau effect characteristic of LFP batteries, which presents a unique challenge for accurately estimating OCV in this region. This effect often leads to reduced voltage variation with changing SOC, providing an ideal condition to test the robustness of the model. Therefore, four data sets will be examined: the APR battery at 60% SOC, which was used for training the model, the APR battery at 50% SOC to verify the model when battery characteristics are known, and the BSE battery at 60% and 50% SOC for which the specific characteristics are unknown.

By monitoring the batteries for 24 hours and using the stopping condition, the true OCV was obtained. Furthermore, these values were compared with the calculated OCV values. The results obtained are presented in Tables IV-2 and IV-3.

Tabel IV-1. Results obtained for OCV calculated after discharge.

Discharge	APR 60%	APR 50%	BSE 60%	BSE 50%
$U_{initial}$	3.266 V	3.261 V	3.244 V	3.244 V
U_{knee}	3.285 V	3.282 V	3.284 V	3.285 V
Calculated OCV	3.2555 V	3.2529 V	3.2571 V	3.2581 V
True OCV	3.294 V	3.292 V	3.296 V	3.294 V
Relative error	1.168%	1.187%	1.179%	1.087%

Tabel IV-2. Results obtained for OCV calculated after charge.

Charge	APR 60%	APR 50%	BSE 60%	BSE 50%
$U_{initial}$	3.357 V	3.348 V	3.409 V	3.397 V
U_{elbow}	3.313 V	3.308 V	3.317 V	3.312 V
Calculated OCV	3.3001 V	3.2952 V	3.2979 V	3.2934 V
True OCV	3.301 V	3.299 V	3.304 V	3.302 V
Relative error	0.027%	0.113%	0.183%	0.257%

The obtained results demonstrate that the model successfully calculates the OCV, having a relative error of less than 0.26% when the batteries were subjected to the charging process and an error below 1.2% after discharge.

The approximation of the state of charge (SOC), in 10% increments, was achieved based on an experimentally obtained dataset by applying a complete charge-discharge cycle and using the aforementioned algorithm for two LFP batteries with different capacities: 1100 mAh (APR) and 1500 mAh (BSE), as shown in Tables IV-4 and IV-5.

Tabel IV-3. Experimental data LFP battery - APR 1100mAh.

SOC	100%	90%	80%	70%	60%	50%	40%	30%	20%	10%
OCV	3.455	3.3345	3.3249	3.302	3.2905	3.2849	3.2684	3.2425	3.2039	3.0987

Tabel IV-4. Experimental data LFP battery - BSE 1500mAh.

SOC	100%	90%	80%	70%	60%	50%	40%	30%	20%	10%
OCV	3.385	3.3347	3.3178	3.3007	3.2879	3.281	3.274	3.2591	3.2312	3.181

The area of interest where the characteristic polynomial should have the smallest error is within the 40% - 80% SOC range due to the plateau region characteristic of LFP batteries, as well as within the 80% SOC – 100% SOC range because of the way these batteries will be stored. As can be observed, the 5th-order polynomial has the lowest errors across the entire range of values. Of course, a higher-order polynomial would result in even smaller errors, but it would also introduce computational challenges and overfitting of the characteristic. Additionally, increasing the order of the characteristic polynomial also increases the computational precision required to determine the state of charge. Therefore, by making a compromise between complexity and error values, the characterization of the two batteries will be done using a 4th-order polynomial, as presented in equations (5) and (6):

$$SOC_{APR} = 100 \cdot (-811.7697719713 \cdot OCV^4 + 10522.49141675 \cdot OCV^3 - 51114.3955091 \cdot OCV^2 + 110282.823738 \cdot OCV^1 - 89174.20659453) \quad (5)$$

$$SOC_{BSE} = 100 \cdot (-1009.059039778 \cdot OCV^4 + 12882.06204957 \cdot OCV^3 - 61607.4321747 \cdot OCV^2 + 130810.64900675 \cdot OCV^1 - 104045.77925049) \quad (6)$$

After all the batteries have been tested, groups of batteries are formed in increments of 10 mΩ starting from the battery with the lowest resistance. Furthermore, for each formed group, the mean value and standard deviation are calculated according to equations (7) and (8).

$$\bar{x} = \frac{x_1 + x_2 + \cdots + x_n}{n} \quad (7)$$

where $\bar{\boldsymbol{x}}$ is the average value of the data set, $\boldsymbol{x_1 + x_2 + \cdots + x_n}$ represents each value from the data set, and $\boldsymbol{n}$ is the number of elements.

$$s = \sqrt{\frac{\sum(x_i - \bar{x})^2}{n - 1}} \quad (8)$$

where s standard deviation, and x_i represents each value from the data set.

Next, it is checked whether the batteries within the same group exceed the previously calculated standard deviation, and if so, they are removed from the group. After all groups have been verified and the non-conforming batteries eliminated, the actual sorting stage is applied to a single battery from the group, which is the closest to the mean value, using one of the methods described in the literature. The state of health obtained for this battery will characterize the entire group, thereby reducing the total testing time.

Based on the state of charge of the two tested batteries, it will be determined which battery will receive a charging impulse and which will receive a discharging impulse. Thus, the battery with the lower state of charge will receive a charging impulse, while the one with the higher state of charge will receive a discharging impulse. At the end of the measurement process, each battery receives an identifier consisting of three elements:

- a unique identification number regarding the battery's chemistry and the serial number within the measurement process;
- the state of charge of the battery determined from the developed model;
- the internal resistance determined after the test is completed.

IV.4 Global evaluation method

The technological flow of the global method for evaluating the state of health of batteries withdrawn from use in the automotive industry unfolds as follows: initially, the voltage at the battery terminals is measured, which is assimilated as the open-circuit voltage (OCV) - this assumption is validated by presuming that the tested batteries have been inactive for more than an hour; after this stage, the open-circuit voltage value is used to estimate the state of charge (SOC) based on the developed model; with the information regarding the state of health of the batteries, it can be further determined which battery will be discharged and which will be charged, thus determining the current direction and its value; the recommended current pulse for the internal resistance determination method is 0.25 C and lasts for 18 seconds, and then the internal resistance of the batteries can be easily determined by applying Ohm's law; after completing the test and calculating the internal resistance, the batteries are coded according to the previously presented procedure and grouped in intervals of 10 mΩ. For each formed battery group, a statistical analysis will be applied to determine the mean value and the standard deviation. Batteries whose internal resistance exceeds the standard deviation will be removed from the group and considered outliers. Conversely, the battery with the internal resistance value closest to the mean will be subjected to a slow method (EIS, NN, FL, GPR, etc.) for determining the state of health, thus characterizing the entire battery group. In this way, the overall testing time of the batteries is significantly reduced by subjecting only one battery from a group to a slow but highly accurate evaluation.

V. Contributions to the structure of the sorting system

The proposed structure utilizes two batteries for testing. One battery is used as a power source, to which a discharge pulse will be applied, and the other battery is used as a load, to which a charge pulse will be applied. Thus, the system allows the simultaneous testing of 2N batteries. Moreover, the flexibility of the proposed system allows the control logic to be adapted and expanded as needed. The proposed system complies with the general framework of systems used in this field and is presented in Figure V-1.

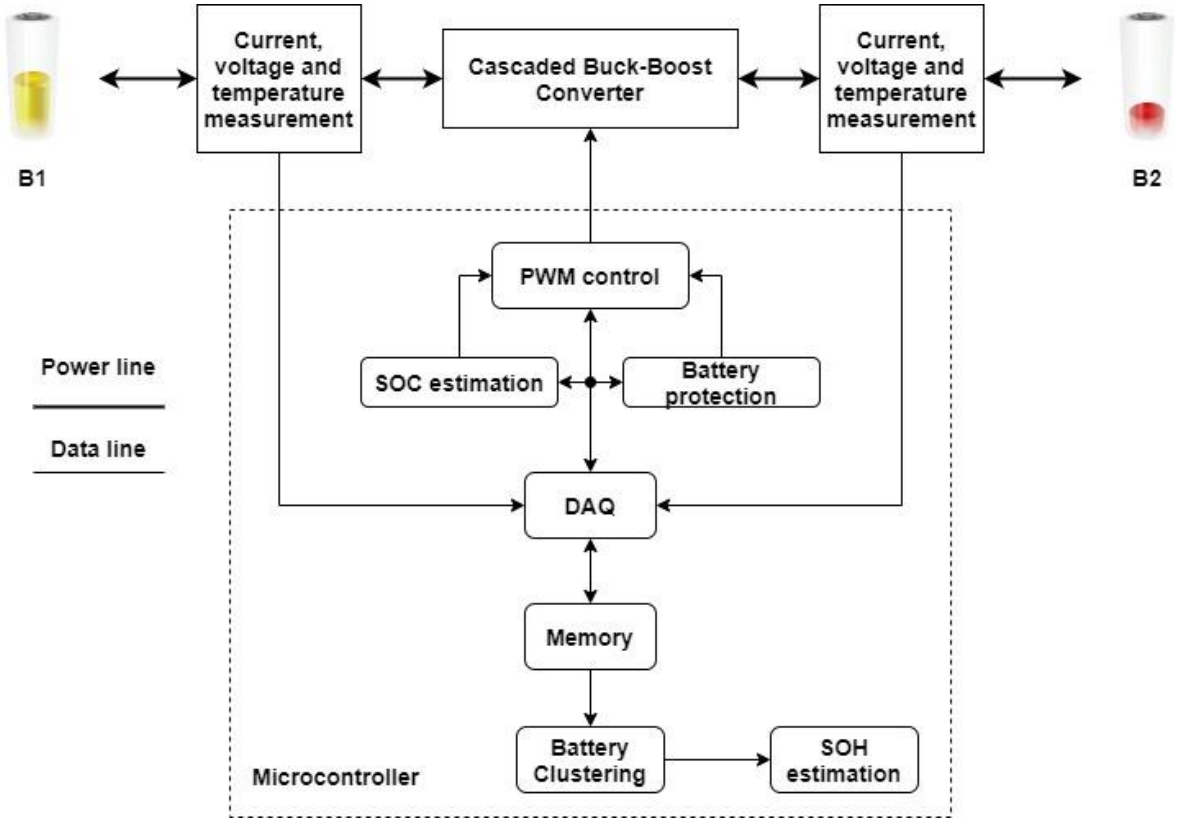

Figura. V-1. Block diagram of the proposed system for determining the SOH of retired batteries.

Based on input parameters and data acquired from sensors, the microcontroller calculates the state of charge (SOC) of the batteries and determines the testing profile and the value of the charge/discharge current pulse or the charging voltage appropriate for the battery chemistry. Additionally, the microcontroller must ensure the proper and safe operation of the system throughout the testing process in cases of overcharging, overdischarging, overheating, short circuits, or other failure causes.

After the testing procedure is completed, the obtained data is analyzed and the batteries are grouped to ensure the group is as homogeneous as possible, meaning that the batteries in the same

group will have very similar characteristic parameters. Finally, the batteries that are not rejected due to inconsistency are evaluated to determine their state of health (SOH) (SOH) [67], [68].

V.1 Cascaded Buck-Boost power converter design

Due to the increasing demand for smart devices that integrate safe battery charge and discharge management, bidirectional DC-DC converters have become a topic of interest in the literature. These converters can maintain the battery within optimal parameters and even extend its operating time [69]. Typically, the charge-discharge process is carried out with two separate circuits, but to reduce size and cost, this process can be integrated into a single circuit. The cascaded Buck-Boost converter allows energy transfer in both directions with the possibility of stepping up or stepping down the voltage, as shown in Figure V-2. The advantage of this structure is its flexibility and high efficiency, up to 97% [70], [71].

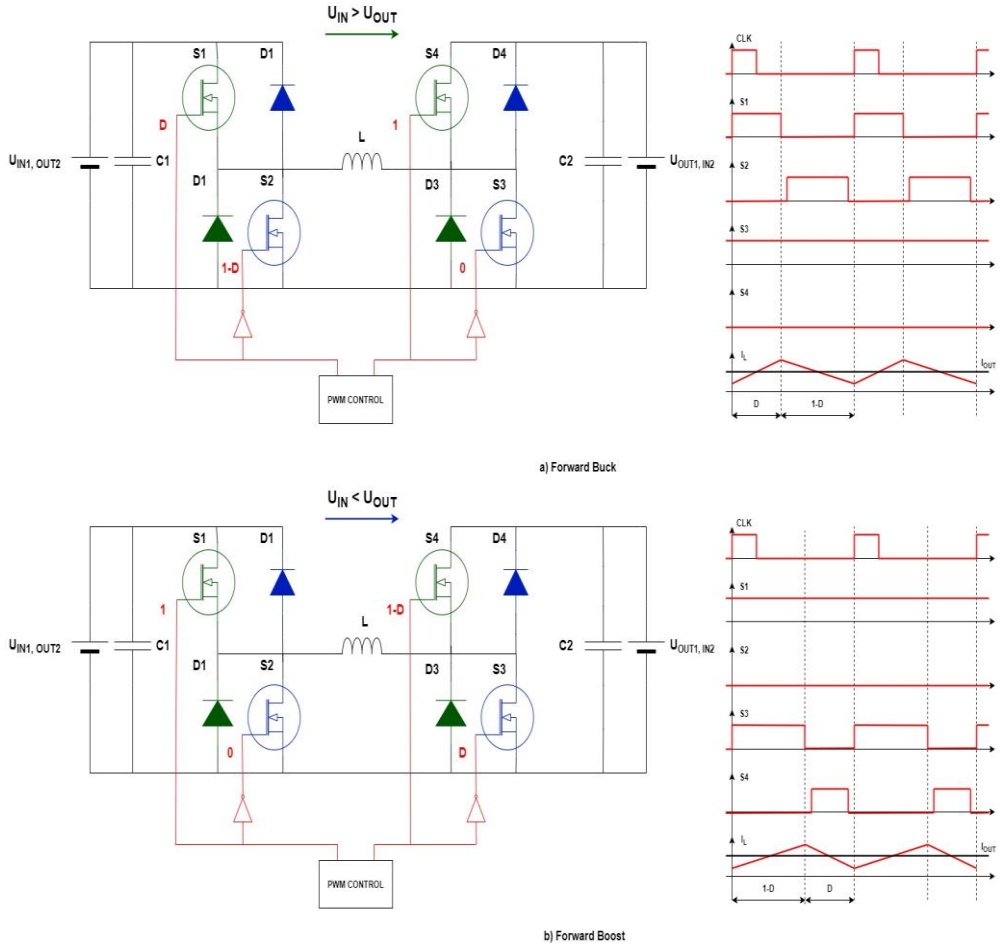

Figura. V-2. The operation principle of the non-isolated Cascaded Buck-Boost bidirectionl DC-DC converter a) Buck operation – Quadrant I; b) Boost operation – Quadrant I.

The control logic for the five operating scenarios, depending on the voltage values and state of charge, is defined in Table V-1. As seen, energy transfer can occur in both directions, with the possibility of operating the converter in Buck (step-down) or Boost (step-up) mode.

Tabel V-1. DC-DC bidirectional Cascaded Buck-Boost converter operating modes depending on voltage difference and battery state of charge.

Voltage condition	**SOC condition**	**Operation mode**	**S1**	**S2**	**S3**	**S4**
$V_{IN} > V_{OUT}$	$SOC_{BAT1} > SOC_{BAT2}$	Buck ($V_{IN1} \rightarrow V_{OUT1}$)	D	1-D	0	1
$V_{IN} > V_{OUT}$	$SOC_{BAT1} < SOC_{BAT2}$	Boost ($V_{IN1} \leftarrow V_{OUT1}$)	1-D	D	0	1
$V_{IN} < V_{OUT}$	$SOC_{BAT1} > SOC_{BAT2}$	Boost ($V_{OUT2} \rightarrow V_{IN2}$)	1	0	1-D	D
$V_{IN} < V_{OUT}$	$SOC_{BAT1} < SOC_{BAT2}$	Buck ($V_{OUT2} \leftarrow V_{IN2}$)	1	0	D	1-D
$V_{IN} \cong V_{OUT}$	$SOC_{BAT1} \cong SOC_{BAT2}$	Buck ($V_{IN1} \rightarrow V_{OUT1}$)	D	1-D	0	1

For circuit design, the specifications need to be specified. Table V-2 presents the input characteristics for designing the electrical and electronic elements. For all the obtained results, the most extreme case will be considered, and components will be chosen to ensure the safe and correct operation of the cascaded bidirectional Buck-Boost converter.

Tabel V-2. Specifications of DC-DC bidirectional Cascaded Buck-Boost converter.

Specifications	**Value**	**Unit**	**Description**
V_{IN_MAX}	14.5	[V]	Maximum input DC value
V_{IN_MIN}	2.5	[V]	Minimum input DC value
f_{SW}	128000	[Hz]	Switching frequency
V_{OUT_MAX}	14.5	[V]	Maximum output DC value
V_{OUT_MIN}	2.5	[V]	Minimum output DC value
I_{OUT}	1	[A]	Maximum output current
Δi_L	10	[%]	Current ripple
Δv_{OUT}	5	[%]	Voltage ripple
$V_{SW\_MAX} = V_{IN\_MAX}$	14.5	[V]	Maximum switching voltage

$I_{SW\_MAX} = I_{OUT}$	1	[A]	Maximum switching current
Randament estimat	90	[%]	Efficiency

The equations for calculating the elements follow the design procedure presented in [72], [73], [74] to design a cascaded bidirectional DC-DC Buck-Boost converter operating in Continuous Conduction Mode (CCM). Considering the results obtained for the chosen elements and their availability at the time of purchase, the following electronic components were selected:

Tabel V-3. The components chosen to develop the Cascaded Buck-Boost converter.

Component type	**Name**	**Supplier**	**Characteristics**	**No. of elements**
Inductor [75]	74437529203221	Wurth Elektronik	$L = 220 \pm 20\%\mu H$ $I_L = 8.8A$	1
Capacitor [76]	875115655003	Wurth Elektronik	$C = 100 \pm 20\%\mu F$ $V_{MAX\_C} = 35V$	2
Diode [77]	IRF530SPBF	Vishay	$V_{DS} = 100V$ $I_{Smax} = I_{F\_AVG} = 14A$	4
MOSFET [77]				
Driver MOSFET [78]	LTC4444	Linear Technology	$V_{IN} = 0 - 100V$ $I_{max} = 2.5A$	2
Capacitor for Driver [79]	T499A224K035ATE18K	Kemet	$C = 0.22 \pm 10\%\mu F$ $V_{MAX\_C} = 35V$	2
Schottky diode for Driver [80]	RB075BGE40S	Rohm	$V_{RRM} = 40V$ $I_{AVG} = 5A$	

Since the current and voltage of the MOSFET command exceed the capabilities of the PWM pins for most control circuits, it was necessary to choose a driver specifically designed for controlling a bridge arm.

V.2 Electronic subsystem simulation for Cascaded Buck-Boost power converter

To test the designed circuit, we used the LTspice XVII program, a high-performance SPICE simulation software capable of visualizing waveforms based on real models of analog and integrated circuits. To achieve the highest quality results, the macromodels of the used elements implement the specifications of the electrical and electronic components chosen in Table V-3. Figure V-3 shows the power circuit diagram simulating the operation of the cascaded bidirectional DC-DC Buck-Boost converter. The control scheme is implemented using two sources that generate a PWM signal necessary for generating the control parameters provided by the power drivers. The analysis of the circuit's operation is based on eight scenarios that address the limitations of the circuit's functioning:

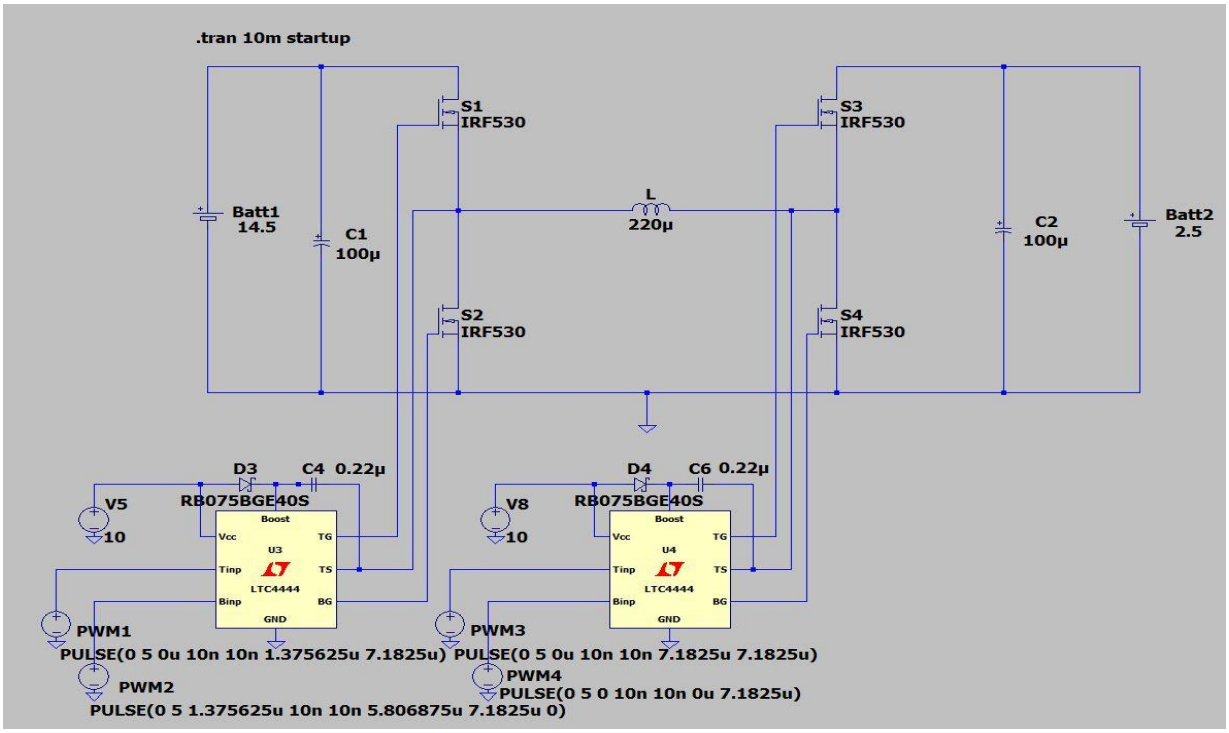

Figura. V-3. Implemented scheme in LTspice XVII for DC-DC bidirectional Cascaded Buck-Boost converter.

V.3 Simulation of the operation of the sorting system

The LTspice program allowed the evaluation of the system in terms of the behavior of integrated circuits and passive circuit elements. However, the real behavior of the batteries could not be replicated, as there was only a generic model for inserting the supplied voltage and the RC parasitic component. Therefore, the study of the system from the perspective of battery behavior

was approached by implementing them using the functional blocks available in Matlab/Simulink. This program allows for the modeling, simulation, and analysis of dynamic systems. Predefined blocks can be used to model linear or nonlinear systems, continuous or discrete in time. Figure V-4 presents the Simulink model used for studying the system for determining the state of health of batteries retired from the automotive industry.

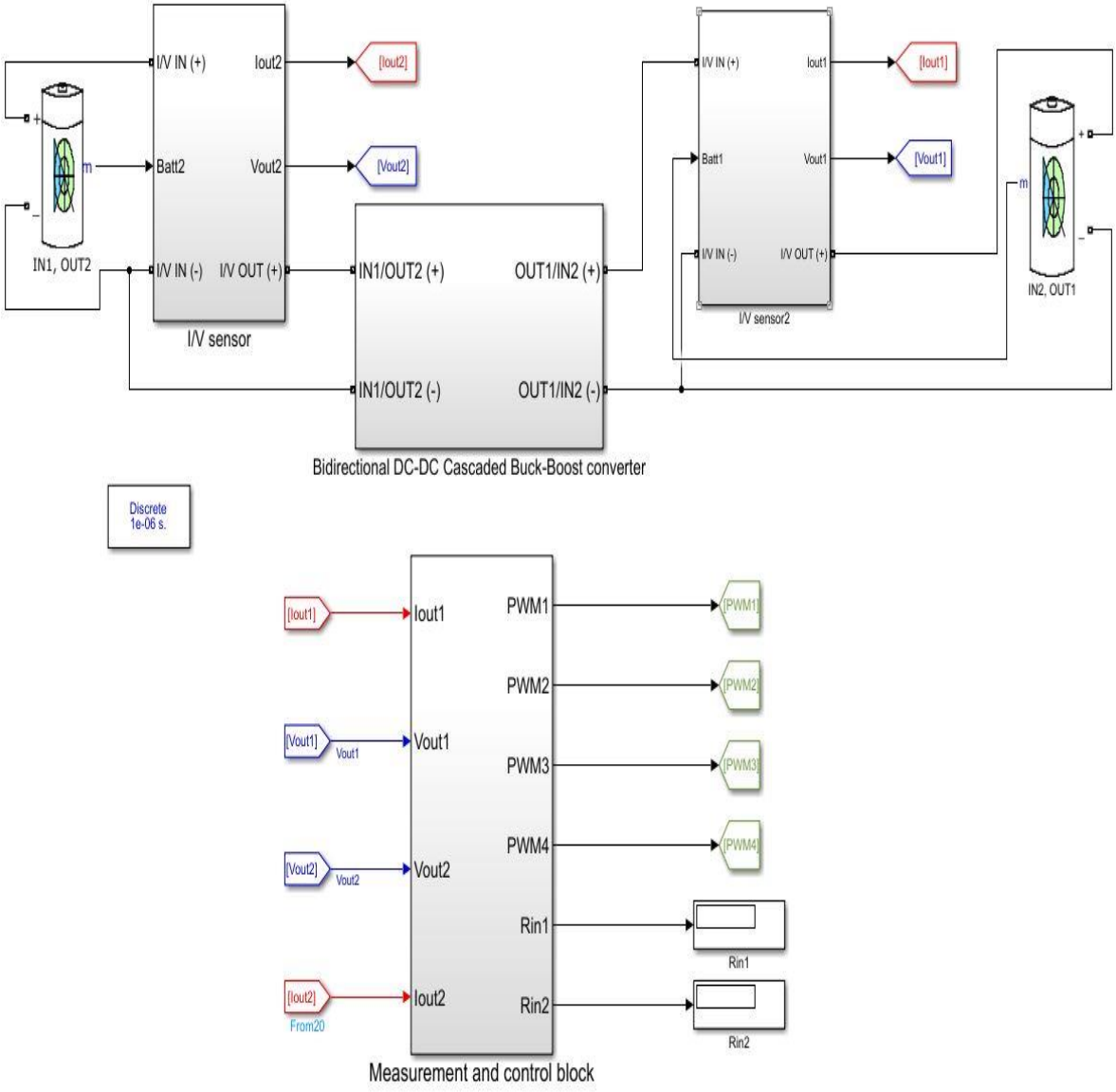

Figura. V-4. Functional block diagram of the proposed system implemented in Matlab/Simulink.

To determine the experimental data necessary for modeling the batteries in MATLAB/Simulink, which implements the Shepherd model, data was acquired from two batches, each consisting of five batteries from different manufacturers (APR and BSE). According to the procedure presented in the USABC manual, the discharge curves at C1/1, C2/2, and C3/3 were

determined, as well as the actual capacity of each battery [52]. he procedure was applied with laboratory equipment three times for a single battery at a temperature of 23°C±2°C. The battery capacity is considered stable when three successive C3/3 discharges present a maximum tolerance of 2%. The capacity is determined using the following relationship:

$$C_{ef} = I_{dchg} \cdot t_{dchg} \; [Ah] \tag{9}$$

where C_{ef} is the actual capacity [Ah], I_{dchg} is the discharge current [A], și t_{dchg} is the discharge time until the battery reach the cut-off voltage [s].

Thus, the characteristic points in the C3/3 discharge curve were extracted to meet the unknown parameters described in equation (10) and implemented in the battery model to obtain a realistic behavior during the simulations. According to [81], the Shepherd model implements the electrochemical behavior of a battery and can be described as follows:

$$V = E_0 - K \cdot \left(\frac{Q}{Q - it}\right) \cdot i - R \cdot i + A \cdot E^{(-B \cdot it)} \tag{10}$$

where E_0 is the open circuit voltage (OCV) at maximum capacity [V], K is the polarization resistance coefficient [Ω], Q is the battery capacity [Ah], i is the current of the battery [A], R is the internal resistance, it is the discharge capacity [Ah], A and B are empirical constants [V], [1/Ah].

Shepherd's equations for battery modeling require a limited number of parameters that can be obtained from the battery manufacturer's data or based on an experimental data set. Moreover, these equations are already part of the battery model found in the Matlab/Simulink program, and therefore, the proposed algorithm can be extended for any technology by introducing the coordinates of the marked points from the nominal discharge characteristic [82], [83].

For conducting the experiments, the following equipment was used: a programmable DC power supply to implement the CC/CCCV charging profile; a programmable DC electronic load to implement the discharge profiles; a thermal chamber to ensure the testing conditions proposed by the manufacturer; a high-resolution data acquisition system; a specialized circuit designed for measuring the state of charge; and a personal computer for creating the control software for the data acquisition board, as shown in Figure V-5.

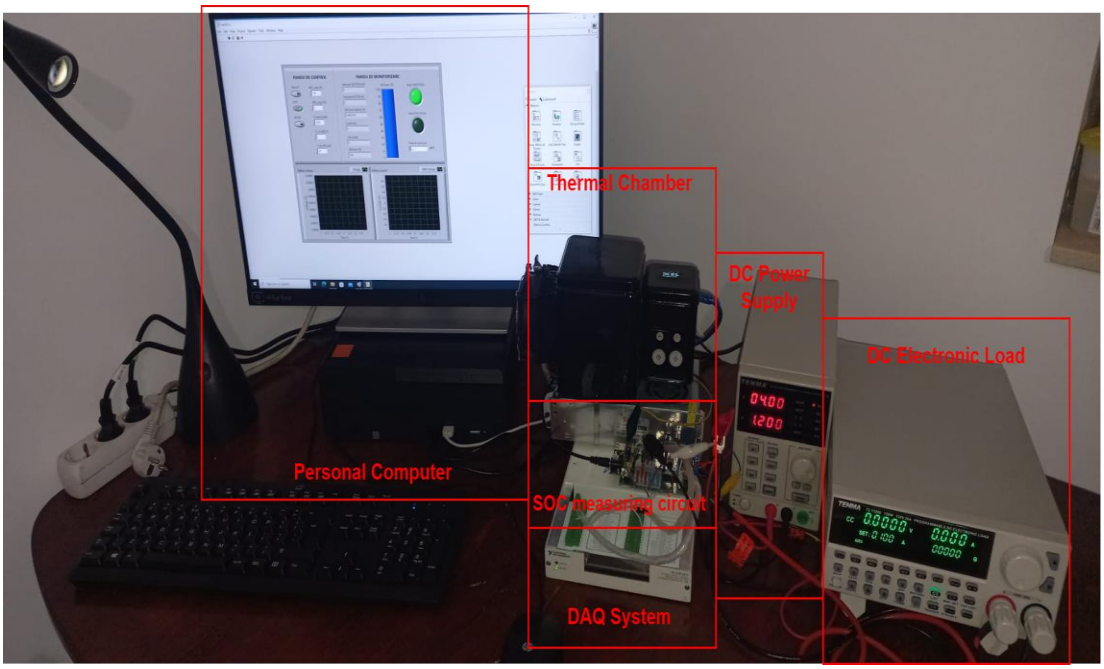

Figura. V-5. Assembly diagram for developing the experiments.

After calculating the actual capacity, it was necessary to verify, according to the USABC manual, if the difference between the obtained value and the nominal value is greater than 2%. If an error greater than 2% is identified, the batteries will be removed from the study.

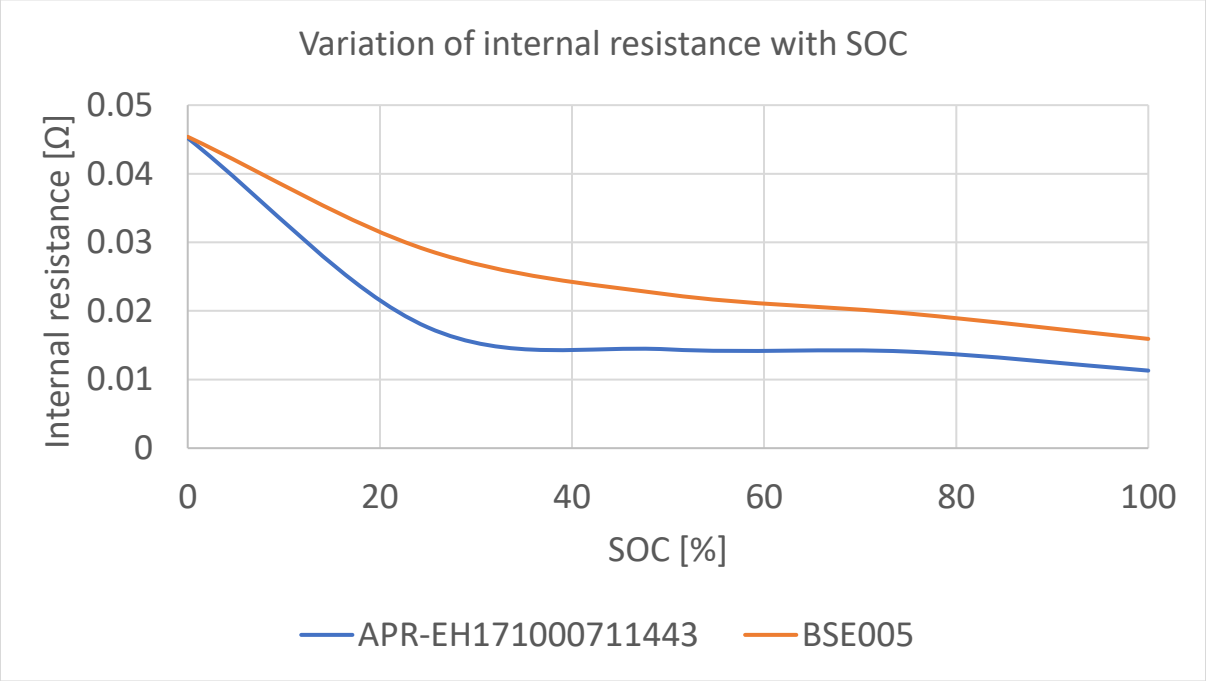

Figura. V-6. Variation of internal resistance with SOC for BSE005 and APR-EH171000711443 batteries.

Figure V-6 presents the results obtained for the internal resistance of APR and BSE batteries at different SOC levels. As the SOC decreases, the internal resistance of the batteries increases, as expected. At 75% SOC, there is an increase in internal resistance of approximately 25% for both batteries compared to the initial value, and a difference of approximately 10-17% between 75% SOC and 50% SOC. At 25% SOC, the internal resistance is 55% higher than the initial value for the APR battery and 300% higher at the end of its lifespan, while the BSE battery shows an increase of about 80% and 185% for the same SOC levels. It is noteworthy that the transient effect at the beginning of the simulation was eliminated by acquiring the OCV at 0.125 seconds.

V.4 Design of test board for force circuit

Considering the promising results obtained through simulation, the printed circuit board (PCB) schematic was further developed, as shown in Figure V-7, using Autodesk Fusion 360, an electrical circuit design program. This software offers a variety of options, including 2D modeling, 3D modeling, generative design, failure mode simulation, electrical and PCB design, production project development, and dynamic scene creation.

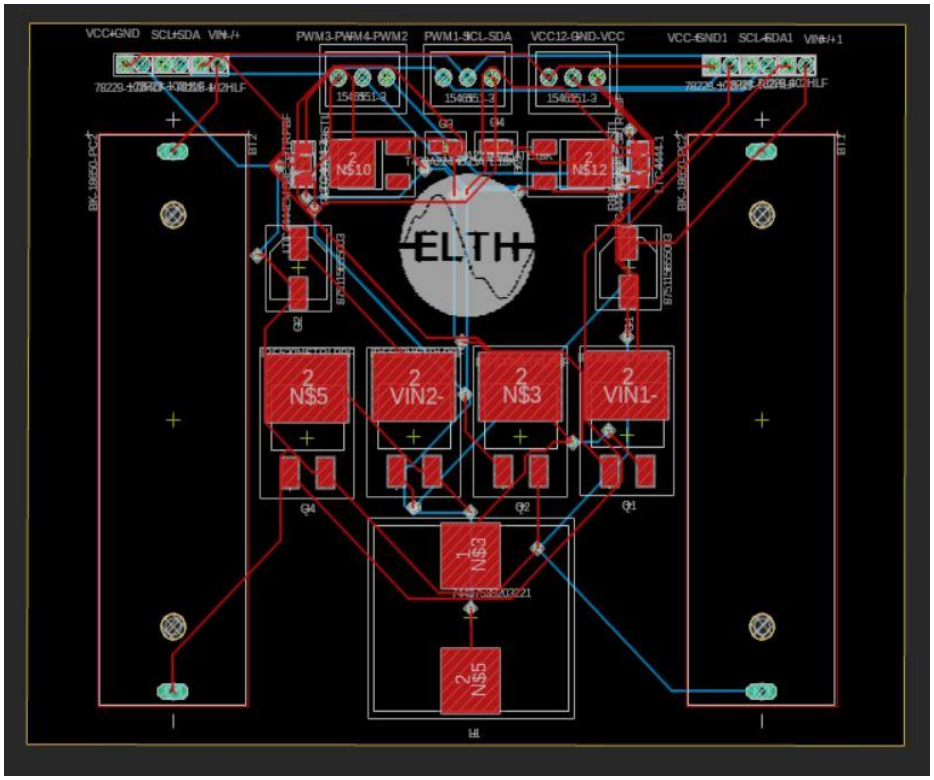

Figura. V-7. The printed circuit board (PCB) resulting from the implementation of the electrical scheme.

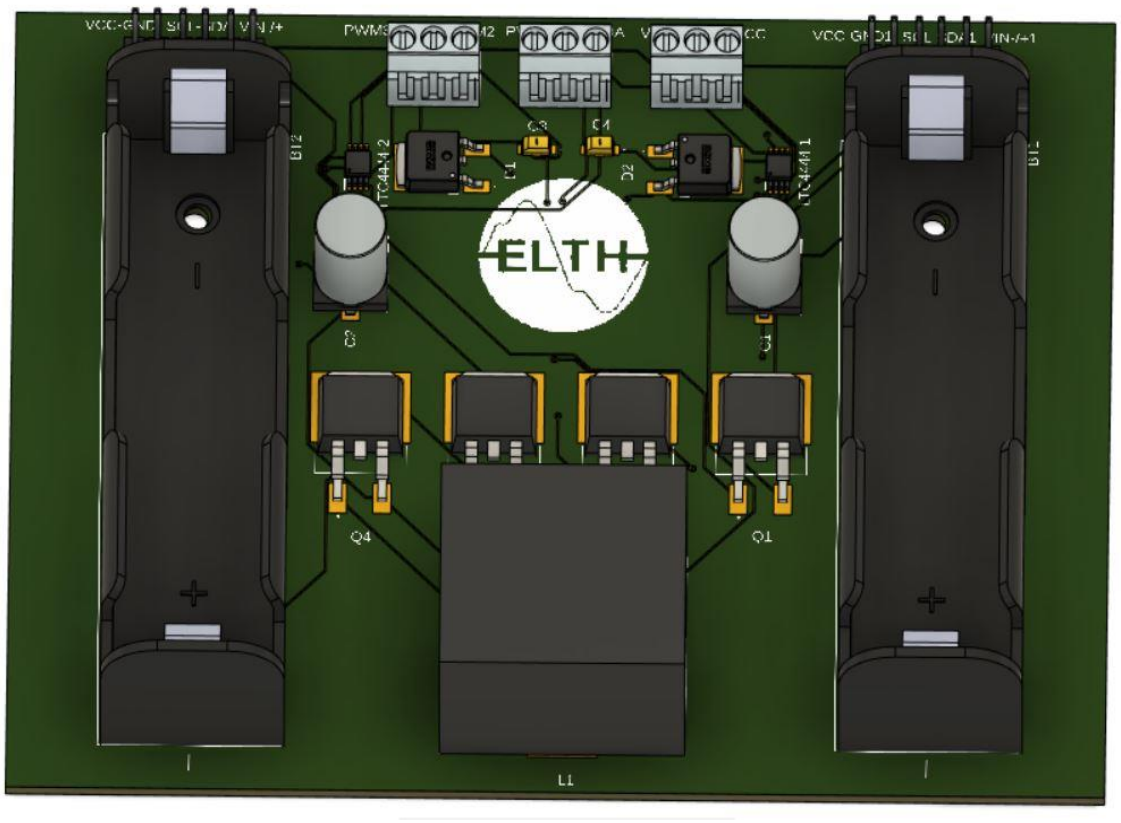

Figura. V-8. Viewing the force scheme in 3D format.

Figure V-8 allows for the visualization of the test board and the placement of components in a 3D format. Generating the circuit in three-dimensional format streamlines the design phase by providing a clear perspective of the designed circuit and identifying possible component placement errors.

V.5 Realization of the command and control system

The control element is implemented using a microcontroller, which is responsible for data processing, battery monitoring, and controlling the power circuit. Additionally, the software program includes protection functions against overcharging, over-discharging, short circuits, etc. The ESP32 microcontroller and other necessary components for user interface implementation, such as an LCD screen and buttons, will be used to develop the control system. This microcontroller was chosen for the following reasons: it allows the generation of very high-frequency PWM signals with a 240MHz clock generator; it has an I2C interface for sensor communication, as well as other communication possibilities (UART, SPI, Wi-Fi, Bluetooth); and it has extended memory for complex developments, with 448kB ROM and 520kB RAM [84]. The electrical schematic of the system is presented in Figure V-9.

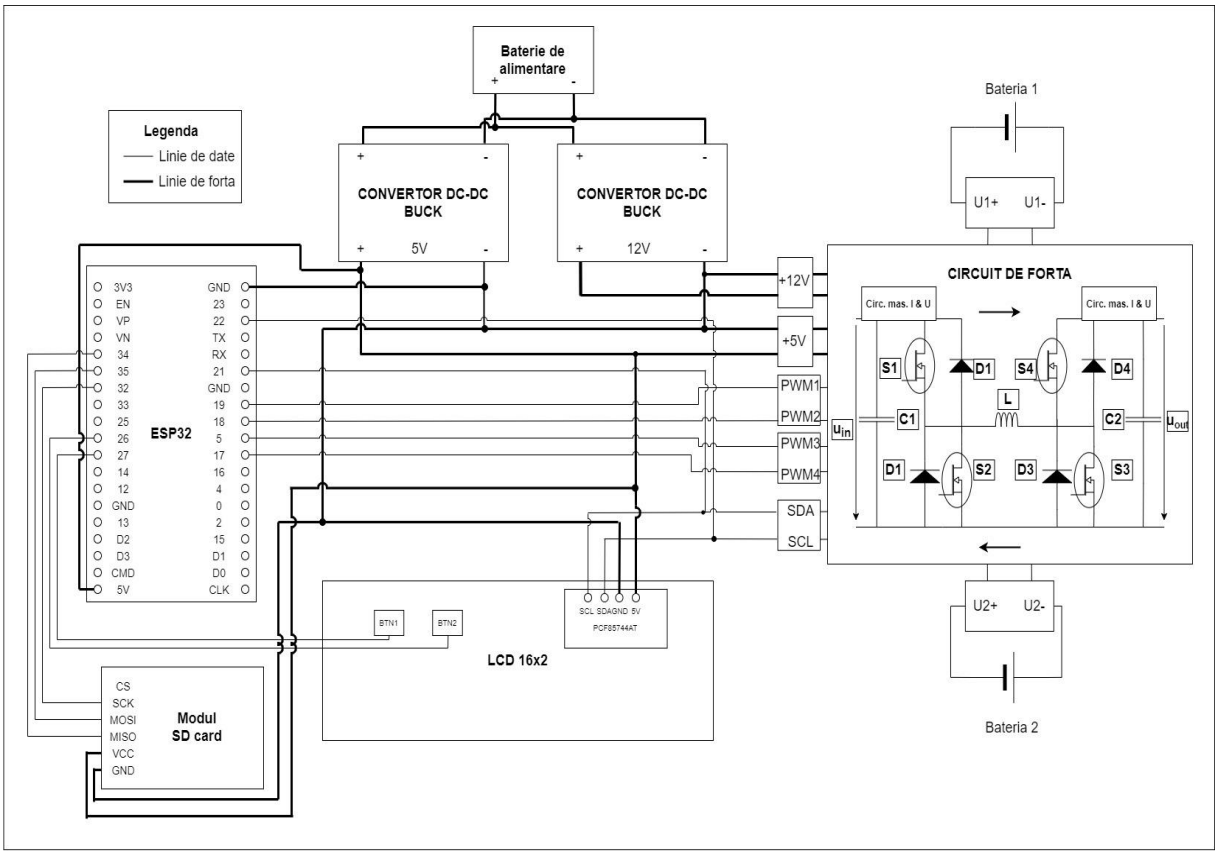

Figura. V-9. Electrical diagram of the proposed system (control circuit and force circuit).

The control logic implemented within the ESP32 microcontroller includes: initializing the testing process via a general switch that powers the entire circuit, also serving as a protection mechanism in case of failure; after activating the general switch, the code sequence calls the corresponding libraries for each component, reads the global variables from ROM memory, and initializes the object configurations. In the main loop of the code, the input/output pins (PWM, SDA, SCL, DAC, ADC) are configured, as well as their state (HIGH, LOW) if necessary, and communication with the devices is established - the test parameter input sequence cannot initialize until the communication is established, and the device will repeat the communication establishment sequence until it is valid. During the initialization phase, the user is prompted to choose the type of test, either DCR Test or Grouping Test, which is then applied until a new test sequence is initiated. The DCR Test sequence evaluates the internal resistance of the batteries and requires the following input parameters: selection of battery chemistry (LFP, NMC, LiPo, etc.) and capacity (900 mAh, 1100 mAh, etc.). Once the test is approved to begin, the first step verifies the capacity range, followed by the pre-testing phase. During this phase, the open-circuit voltage (OCV) measurement function is called to determine the state of charge (SOC) of the batteries based on previously developed models. The current pulse is calculated as C/4 of the capacity, determining which battery will be charged and which discharged, and the operation mode of the

power converter (FW Buck, RE Boost, RE Buck, FW Boost) is set. After this pre-testing phase, an 18-second countdown starts, during which the charge/discharge current pulse is applied. Throughout the pulse duration, the voltage and current of the batteries are monitored. After the countdown ends, the power circuit stops, and data processing begins. In this final stage, the internal resistance of the batteries is calculated, and the saved data is sent to a computer for applying the battery health determination algorithm, or the data is uploaded to an SD card, after which the procedure initialization phase resumes. If the Grouping Test option is selected, meaning after evaluating all the batteries in the working set, the file uploaded to the SD card is accessed, and the battery grouping function is run. The INA219 module, with a 1% measurement accuracy, a 12-bit analog-to-digital converter, and a current measurement resolution of 0.1 mA, is used for current measurement [85]. Additionally, the user interface was created using a 16x2 LCD with buttons for menu navigation and the I2C communication interface [86].

VI. Developing the source code for battery sorting

Before the physical realization of the circuit and the implementation of the control algorithm, the circuit was simulated using the Wokwi platform. This platform is an online electronic emulator that allows the integration and simulation of various electronic components such as ESP32, buttons, the INA219 current and voltage sensor, passive circuit elements, LCDs, etc.

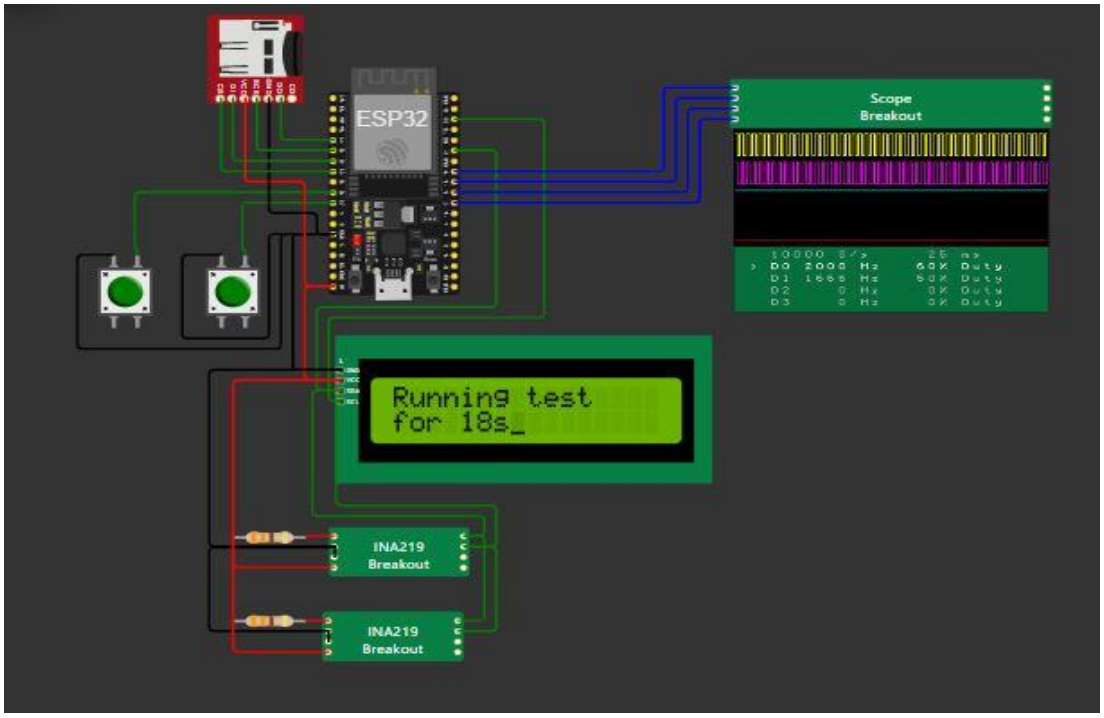

Figura. VI-1. Circuit diagram implemented in Wokwi platform.

The following code was used to determine the SOC-OCV relationship. Initially, the measurement functions of the INA219 sensors are called, and the voltage at the battery terminals is saved, which is considered as the open-circuit voltage (OCV). It is important to note that in this phase of the testing procedure, the power switches are not activated. Next, the state of charge (SOC) of the two tested batteries is determined using the model previously presented. If the determined state of charge exceeds the threshold of 100% or drops below 10%, the value is saturated. Finally, the operation mode of the power converter is determined based on the SOC and OCV of the two batteries, according to the operating scenarios presented earlier.

```
    measurement1(); // acquire OCV from battery 1
    measurement2(); // acquire OCV from battery 2
    OCV1 = loadvoltage1;
    OCV2 = loadvoltage2;
    Serial.print("OCV1 [V]: "); Serial.print(OCV1); Serial.println(" ");
    Serial.print("OCV2 [V]: "); Serial.print(OCV2); Serial.println(" ");
    SOC1 = (-a4*pow(OCV1, 4) + a3*pow(OCV1,3) - a2*pow(OCV1, 2) +
a1*pow(OCV1, 1) - a0);
    SOC2 = (-a4*pow(OCV2, 4) + a3*pow(OCV2,3) - a2*pow(OCV2, 2) +
a1*pow(OCV2, 1) - a0);
    Serial.print("SOC1 [%]: "); Serial.print(SOC1); Serial.println(" ");
    Serial.print("SOC2 [%]: "); Serial.print(SOC2); Serial.println(" ");
    if (SOC1 > SOC_UpLimit) {SOC1 = SOC_UpLimit;}
    if (SOC1 < SOC_LowLimit) {SOC1 = SOC_LowLimit;}
    if (SOC2 > SOC_UpLimit) {SOC2 = SOC_UpLimit;}
    if (SOC2 < SOC_LowLimit) {SOC2 = SOC_LowLimit;}
    if ((SOC1 > SOC2) && (OCV1 > OCV2)) { // FW Buck
      FWbuck = 1;
      Serial.println("Forward Buck"); Serial.println(" ");
    }
    if ((SOC1 < SOC2) && (OCV1 > OCV2)) { // RE Boost
      REboost = 1;
      Serial.println("Reverse Boost"); Serial.println(" ");
    }
    if ((SOC1 > SOC2) && (OCV1 < OCV2)) { // RE Buck
      REbuck = 1;
      Serial.println("Reverse Buck"); Serial.println(" ");
    }
    if ((SOC1 < SOC2) && (OCV1 < OCV2)) { // FW Boost
      FWboost = 1;
      Serial.println("Forward Boost"); Serial.println(" ");
    }
```

VII. Results and conclusions

In the doctoral thesis, several sorting methods for batteries were studied, and following a comparative study that focused on operating time, SOH determination error, advantages, and disadvantages, it was determined that the method based on determining the internal resistance in direct current is the most suitable in terms of operating time and large-scale application. Thus, this method is applied as an intermediate step that groups batteries based on internal resistance, with only one battery from a group being further tested to determine the actual age of the group. Furthermore, a multi-criteria analysis of bidirectional DC-DC power converters was conducted, and it was established that the cascaded Buck-Boost topology represents the optimal solution for creating a testing system that allows rapid evaluation of batteries from different technologies. Therefore, Figure VII-1 presents a top view of the developed prototype.

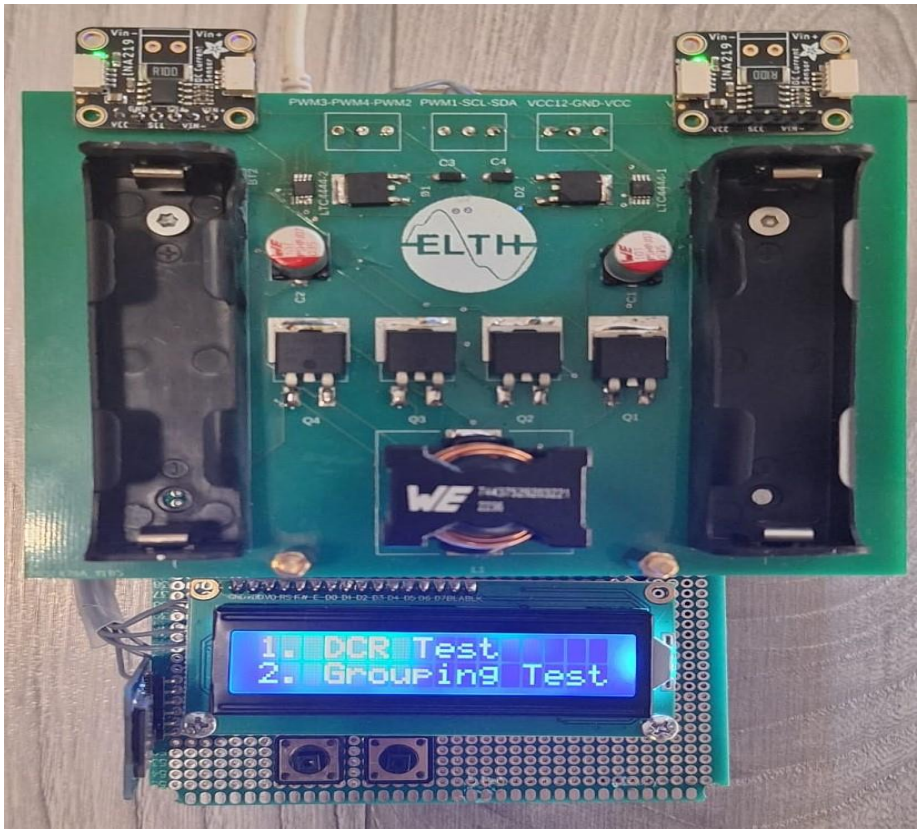

Figura. VII-1. Prototype of the proposed system (top view).

To validate the method and system, ten LFP cells were used, divided into four sub-lots. Initially, the actual capacity was determined according to the procedure described in the USABC manual. Each cell was subjected to a testing sequence consisting of three constant current discharge cycles. A discharge cycle involves using three current values: C3/3, C2/2, and C1/1. After each discharge stage, the battery was left for one hour to stabilize the terminal voltage, and then it was charged according to the manufacturer's specifications using the CCCV method. This

procedure was repeated three times for each battery, and the capacity obtained for the C3/3 cycle was considered the effective capacity of the batteries.

Based on this experimental data, the cells were aged using the testing procedure known as Random Walking [87], [88]. This procedure involves applying a random sequence of discharge and charge currents, each lasting 5 minutes, starting from a fully charged battery. The testing sequence consists of 12 steps for one hour, or 96 steps for one day (8 hours). Figure VII-2 shows the Random Walking discharge profile implemented using a power supply and an electronic load. Initially, a maximum discharge current of -2.25A is applied, and then every 5 minutes, with one-second pauses, the current value becomes -1.875A, -1.5A, -1.125A, -0.75A, and -0.375A, respectively. After this sequence, a charging current is applied, starting from the minimum value to the maximum value.

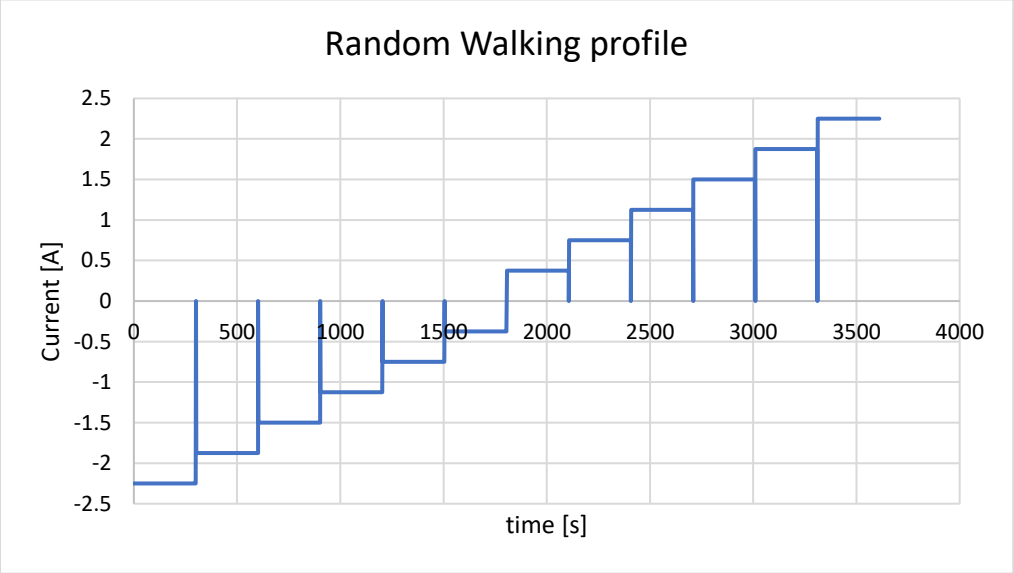

Figura. VII-2. Random Walking profile used for cell aging.

The batch of ten batteries was divided into four sub-lots as follows: batteries APR-EH171000702406 and APR-EH171000707606 are part of the first sub-lot and will be aged to a state of health (SOH) of 95%; batteries APR-EH171000705424 and APR-EH171000711443 will make up sub-lot 2, which will be aged to approximately 92% SOH; batteries APR-EH171000814013, APR-EH171000708804, and APR-EH171000707901 constitute sub-lot 3, which will be aged to approximately 88% SOH; and batteries APR-EH171000714657, APR-EH171000711199, and APR-EH171000701957 will be part of sub-lot 4, which will be aged to approximately 86% SOH. The chosen SOH values were selected to test the proposed system's ability to identify at least four groups of batteries. Additionally, there is a difference of 2%, 3%, and 5% between the chosen SOH thresholds. Following the application of the Random Walking profile, the new SOH values are presented in Table VII-1.

Tabel VII-1. SOH values of aged batteries after applying the Random Walking profile.

Battery ID	Nominal capacity [mAh]	Effective capacity [mAh]	Actual SOH [%]	Sublot
APR-EH171000702406	1100	1053.0	95.72	1
APR-EH171000707606		1049.6	95.41	1
APR-EH171000705424		1009.6	91.78	2
APR-EH171000711443		1015.4	92.30	2
APR-EH171000814013		976.4	88.76	3
APR-EH171000708804		971.9	88.35	3
APR-EH171000707901		966.0	87.81	3
APR-EH171000714657		947.32	86.12	3
APR-EH171000711199		945.01	85.91	4
APR-EH171000701957		944.46	85.86	4

Each testing phase involves checking two batteries with different SOH and SOC values. According to previous discussions, the batteries will be stored as follows: charged according to the storage procedure, with SOC considered at 40%; partially charged after long-term storage, with SOC considered at 80%; and fully charged – SOC 95%-100%. Therefore, the following operating scenarios will be considered for system validation:

1. Scenario 1: Battery 1 SOH 86% - SOC 80%, Battery 2 SOH 88% - SOC 80%, FW Buck operating mode;
2. Scenario 2: Battery 1 SOH 86% - SOC 95%, Battery 2 SOH 95% - SOC 40%, RE Buck operating mode;
3. Scenario 3: Battery 1 SOH 88% - SOC 95%, Battery 2 SOH 92% - SOC 40%, RE Buck operating mode;

4. Scenario 4: Battery 1 SOH 86% - SOC 80%, Battery 2 SOH 92% - SOC 40%, FW Buck operating mode;
5. Scenario 5: Battery 1 SOH 88% - SOC 80%, Battery 2 SOH 95% - SOC 40%, FW Buck operating mode.

To verify the results, two data sets were obtained, Tables VII-2 and VII-3, for which the relative error of the batteries' internal resistance was calculated. The obtained verification data will be used to validate the sorting method.

Tabel VII-2. Experimental data obtained following the application of the algorithm for determining the internal resistance of batteries.

Scenario	**1**	**2**	**3**	**4**	**5**
ID1	LFP1100_001_78_085	LFP1100_003_94_083	LFP1100_005_92_072	LFP1100_007_81_080	LFP1100_009_77_077
ID2	LFP1100_002_80_075	LFP1100_004_41_045	LFP1100_006_37_056	LFP1100_008_40_058	LFP1100_010_39_048
Technology	LFP				
Capacity [mAh]	1100				
Ipulse [A]	$\pm$0.375				
OCV1 [V]	3.319	3.340	3.338	3.323	3.318
OCV2 [V]	3.322	3.267	3.259	3.265	3.263
SOC1 [%]	78.07	94.29	92.77	81.17	77.29
SOC2 [%]	80.40	41.96	37.62	40.84	39.74
Vdt1 [V]	0.032	0.031	0.027	0.030	0.029
Vdt2 [V]	0.029	0.017	0.021	0.022	0.018
Rin1 [Ω]	85.79	83.11	72.39	80.43	77.75

Rin2 [Ω]	75.07	45.45	56.15	58.82	48

Tabel VII-3. Experimental data obtained for checking the internal resistance of batteries.

Scenario	**1**	**2**	**3**	**4**	**5**
ID1	LFP1100_011_78_082	LFP1100_013_94_085	LFP1100_015_92_072	LFP1100_017_78_080	LFP1100_019_78_074
ID2	LFP1100_012_79_077	LFP1100_014_42_048	LFP1100_016_38_058	LFP1100_018_43_056	LFP1100_020_40_045
Tehnology	LFP				
Capacity [mAh]	1100				
Ipulse [A]	±0.375				
OCV1 [V]	3.319	3.34	3.338	3.319	3.319
OCV2 [V]	3.321	3.268	3.26	3.27	3.265
SOC1 [%]	78.07	94.29	92.77	78.07	78.07
SOC2 [%]	79.62	42.53	38.14	43.69	40.84
Vdt1 [V]	0.031	0.032	0.027	0.030	0.028
Vdt2 [V]	0.027	0.018	0.022	0.021	0.017
Rin1 [Ω]	82.67	85.56	72	80.43	74.67
Rin2 [Ω]	77.33	48.13	58.98	56.15	45.33

The results obtained from the second data set will be used for further validation of the grouping method. Therefore, battery groups were formed with 10 mΩ intervals, starting with the battery with the lowest internal resistance, as shown in Table VII-4:

Tabel VII-4. The groups of batteries formed after sorting.

	Battery ID	Internal resistance [mΩ]
Group 1	LFP1100_001_84_085	85.79
	LFP1100_013_94_085	85.56
Group 2	LFP1100_007_81_080	80.43
	LFP1100_009_77_077	77.75
	LFP1100_003_95_083	83.11
	LFP1100_011_78_082	82.67
	LFP1100_012_79_077	77.33
	LFP1100_017_78_080	80.43
Group 3	LFP1100_004_40_045	45.45
	LFP1100_010_39_048	48
	LFP1100_014_42_048	48.13
	LFP1100_020_40_045	45.33
Group 4	LFP1100_006_37_056	56.15
	LFP1100_008_40_058	58.82
	LFP1100_016_38_058	58.98
	LFP1100_018_43_056	56.15
Group 5	LFP1100_005_92_072	72.39
	LFP1100_015_92_072	72
	LFP1100_002_80_075	75.07
	LFP1100_019_78_074	74.67

The obtained ranges are: 45.33-55.33 mΩ, 55.33-65.33 mΩ, 65.33-75.33 mΩ, 75.33-85.33 mΩ, 85.33-95.33 mΩ. Thus, the batteries were sorted into five different groups. For each group, the mean value and standard deviation were calculated to check for any gross errors outside the $\pm\sigma$ range. After this stage, the battery with the internal resistance closest to the mean value was identified, so that only one battery would be subjected to the SOH evaluation process. The results are presented in Table VII-5.

Tabel VII-5. Results obtained after applying the grouping method.

	Group 1	Group 2	Group 3	Group 4	Group 5
Average [mΩ]	85.67	80.28	46.72	57.52	73.53
Standard deviat	0.16	2.40	1.54	1.58	1.56

ion [mΩ]					
Range of values [mΩ]	85.51-85.83	77.88-82.68	45.18-48.27	55.93-59.11	71.97-75.09
Accepted batteries	LFP1100_001_84_085 LFP1100_013_94_085	LFP1100_007_81_080 LFP1100_003_95_083 LFP1100_011_78_082 LFP1100_017_78_080	LFP1100_004_40_045 LFP1100_010_39_048 LFP1100_014_42_048 LFP1100_020_40_045	LFP1100_006_37_056 LFP1100_008_40_058 LFP1100_016_38_058 LFP1100_018_43_056	LFP1100_005_92_072 LFP1100_015_92_072 LFP1100_002_80_075 LFP1100_019_78_074
SOH range [%]	86	86-88	95	92	88
Battery closest to average	LFP1100_001_84_085 LFP1100_013_94_085	LFP1100_007_81_080 LFP1100_017_78_080	LFP1100_014_42_048	LFP1100_006_37_056 LFP1100_018_43_056	LFP1100_005_92_072

The dependency between SOC and OCV is independent of SOH, and the dependency between SOH and Rin is independent of SOC, so one of the variables must be known. Thus, SOC and Rin are determined according to the previously presented procedure, and based on the state of charge, the internal resistance at the current SOC and at 100% SOC is estimated. The difference between the two is then added to the measured internal resistance. The new internal resistance, corresponding to 100% SOC and the current SOH, is compared to the internal resistance at 100% SOC and SOH. If the internal resistance is greater than that at 100% SOH after the comparison, then the method is validated, confirming that the studied battery has a different SOH than 100%. For modeling the dependency between internal resistance and state of charge, a linear regression with a third-order polynomial was used to approximate the trend during both charging and discharging, as shown in Figure VII-3.

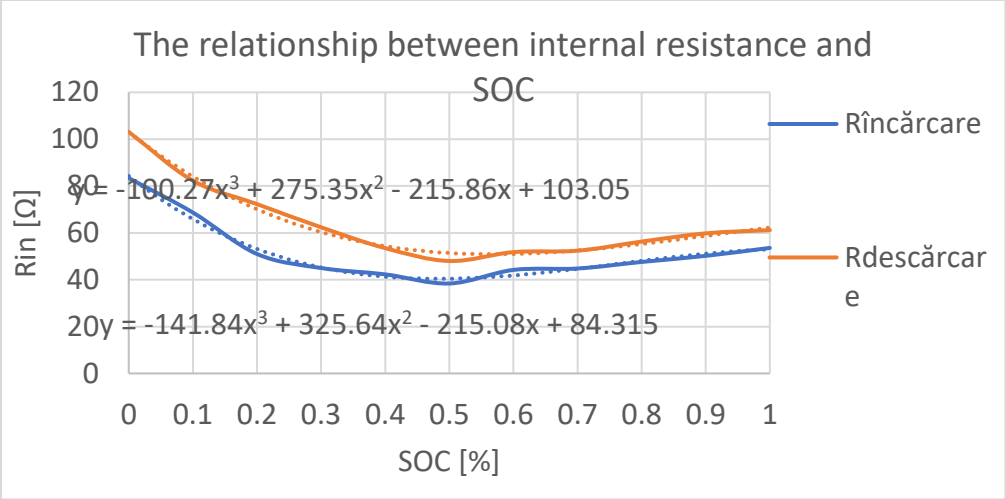

Figura. VII-3. The model made to estimate the internal resistance.

The characteristic equations for the internal resistance model for loading and unloading, respectively, are presented in equations (11) and (12):

$$R_{dchg} = -100.27 \cdot SOC^3 + 275.35 \cdot SOC^2 - 215.86 \cdot SOC + 103.05 \quad (11)$$

$$R_{chg} = -141.84 \cdot SOC^3 + 325.64 \cdot SOC^2 - 215.08 \cdot SOC + 84.315 \quad (12)$$

By applying the two equations for the first group of batteries LFP1100_001_84_085 and LFP1100_013_94_085 we get:

$$R_{dchg} = -100.27 \cdot 0.94^3 + 275.35 \cdot 0.94^2 - 215.86 \cdot 0.94 + 103.05 = 56.58\ m\Omega \quad (13)$$

$$R_{chg} = -141.84 \cdot 0.84^3 + 325.64 \cdot 0.84^2 - 215.08 \cdot 0.84 + 84.315 = 52.06\ m\Omega \quad (14)$$

For 100% SOC the internal resistances will be:

$$R_{dchg} = -100.27 \cdot 1^3 + 275.35 \cdot 0.1^2 - 215.86 \cdot 1 + 103.05 = 62.27\ m\Omega \quad (15)$$

$$R_{chg} = -141.84 \cdot 1^3 + 325.64 \cdot 1^2 - 215.08 \cdot 1 + 84.315 = 53.03\ m\Omega \quad (16)$$

The difference between the resistors becomes:

$$\Delta R_{dchg} = 62.27\ m\Omega - 56.58\ m\Omega = 5.69\ m\Omega \quad (17)$$

$$\Delta R_{chg} = 53.03\ m\Omega - 52.06\ m\Omega = 0.97\ m\Omega \quad (18)$$

Next, this difference is added to the measured values and compared with the estimated values at 100% SOC and SOH:

$$R_{\text{LFP1100\_001\_84\_085}} = 5.69\ m\Omega + 85.79\ m\Omega = 91.48\ m\Omega > 62.27\ m\Omega \quad (19)$$

$$R_{\text{LFP1100\_013\_94\_085}} = 0.97\ m\Omega + 85.56\ m\Omega = 86.53\ m\Omega > 53.03\ m\Omega \quad (20)$$

The validation phase focused on two directions: system validation and sorting method validation. To validate the system, initial tests were conducted to verify the operating modes in the four possible cases using laboratory equipment, followed by real-world operating scenarios to determine experimental data. For the validation of the sorting method, ten new LiFePO4 batteries were analyzed. The actual capacity of the batteries was determined using the procedure presented in the USABC manual to calculate SOH, after which the batteries were divided into four sub-lots and subjected to accelerated aging by applying the Random Walking profile until values close to 86%, 88%, 92%, and 95% SOH were obtained. Subsequently, the internal resistances of the batteries were measured by applying an 18-second charge/discharge current pulse, and a second set of measurements was conducted to verify the obtained data. The grouping method was then applied to the two data sets, resulting in five groups of batteries with different states of charge. To verify the results, a model was created to represent the dependency between SOH and Rin for a battery with 100% SOH, which was used to compare the measured values. The final results indicate the correct identification of battery groups, although three groups contained batteries with 86% and 88% SOH. This result falls within the 2% error margin suggested in the literature and the USABC manual.

VII.1 Personal contributions

Considering the previously discussed, I can state that in this doctoral thesis, personal contributions materialized in three essential directions:

• conceptual: study and analysis of the main methods of sorting batteries withdrawn from the automotive industry, as well as bidirectional DC-DC conversion structures for the realization of sorting systems;

• experimental: creating an own battery sorting system capable of quickly evaluating a wide range of battery technologies;

• technological: expanding the classic method of sorting batteries withdrawn from use by developing a new methodology for grouping batteries; developing a model for determining OCV and SOC-OCV dependence.

Thus, the following objectives were pursued and achieved, which are also original contributions in the field:

1. Elaboration of an extensive study, based on the review of an important number of bibliographic references, regarding the current methods of sorting batteries withdrawn from the automotive industry. This study was carried out in the context of the development of a new sorting

methodology that addresses rapid battery health assessment strategies and facilitates large-scale application.

2. Elaboration of an extensive bibliographic study on bidirectional DC-DC conversion structures in order to establish the optimal topology for the realization of the sorting system that would allow the testing of multi-technology type batteries.

3. Development of a new battery sorting methodology in order to determine the state of health. The new method comprises an intermediate presorting step by which batteries are grouped according to internal resistance and a data processing method obtained using statistical techniques by which a single battery is evaluated and which characterizes between the group.

4. Development of the methodological framework for sorting batteries according to internal resistance.

5. Development of a new method for determining OCV that uses an online observer to identify the inflection point on the voltage curve.

6. Development of a model that approximates the dependence between the state of charge (SOC) of a battery and the open circuit voltage (OCV).

7. Design and choice of power circuit components.

8. Study and simulation of the system in order to analyze the behavior of digital and analog circuits in the specialized program LTspice.

9. Study and simulation of system operation in the Matlab/Simulink program.

10. Adapting and improving the Sheperd analytical model for the functional block in Matlab/Simulink with experimental data.

11. Designing and making the printed circuit board (PCB) and the 3D model in the Autodesk Fusion 360 program.

12. Design and development of the control system to implement the power converter control technique and sorting method.

13. Implementation and verification of the sorting algorithm in the Wokwi platform.

14. Consolidation of the results obtained by testing and validating the sorting system.

15. Development of the methodology in order to expand the solution for testing 2N batteries.

VII.2 Further development directions

To maintain the battery sorting system at the highest technological standards and to extend its capabilities in the future, the following development directions are proposed:

1. Voltage range extension:

Adapting the system to support a wider voltage range will allow for the testing and evaluation of new battery technologies that will appear on the market. This includes batteries with innovative chemistries such as solid-state, lithium-sulfur, and metal-oxygen-based batteries. Expanding the voltage range will ensure system compatibility with a diverse range of batteries, thus facilitating research and development of new energy technologies.

2. Improving the sorting method with AI-based algorithms:

Integrating advanced AI algorithms for the analysis and prediction of battery health can significantly enhance the accuracy and efficiency of the proposed sorting method. Developing a self-learning model that can continuously adapt and improve algorithms based on real-time data will allow the system to learn from previous uses and adjust health assessment methods to optimally reflect the real conditions and behaviors of the batteries.

3. System expansion for testing 2N batteries:

Figure VII-4 shows a solution for expanding the proposed system. Thus, 2N batteries of identical or different technologies can be tested simultaneously, the test time being reduced by half, and at the end of the presorting procedure, 2N internal resistances are obtained. The system can be extended to test 2N batteries, B11-B21, B12-B22 ... B1N-B2N, by mounting in parallel N force modules containing power switches PS11-PS21-PS31-PS41, PS12-PS22- PS32-PS42 ... PS1N-PS2N-PS3N-PS4N, filter capacitors C11-C21, C12-C22 ... C1N-C2N, a magnetic energy storage element L1, L2 ... LN and current sensors and voltage providing the information I11-U11-I21-U21, I12-U12-I22-U22 ... I1N-U1N-I2N-U2N. The command of the N force modules is carried out by the same command and control block.

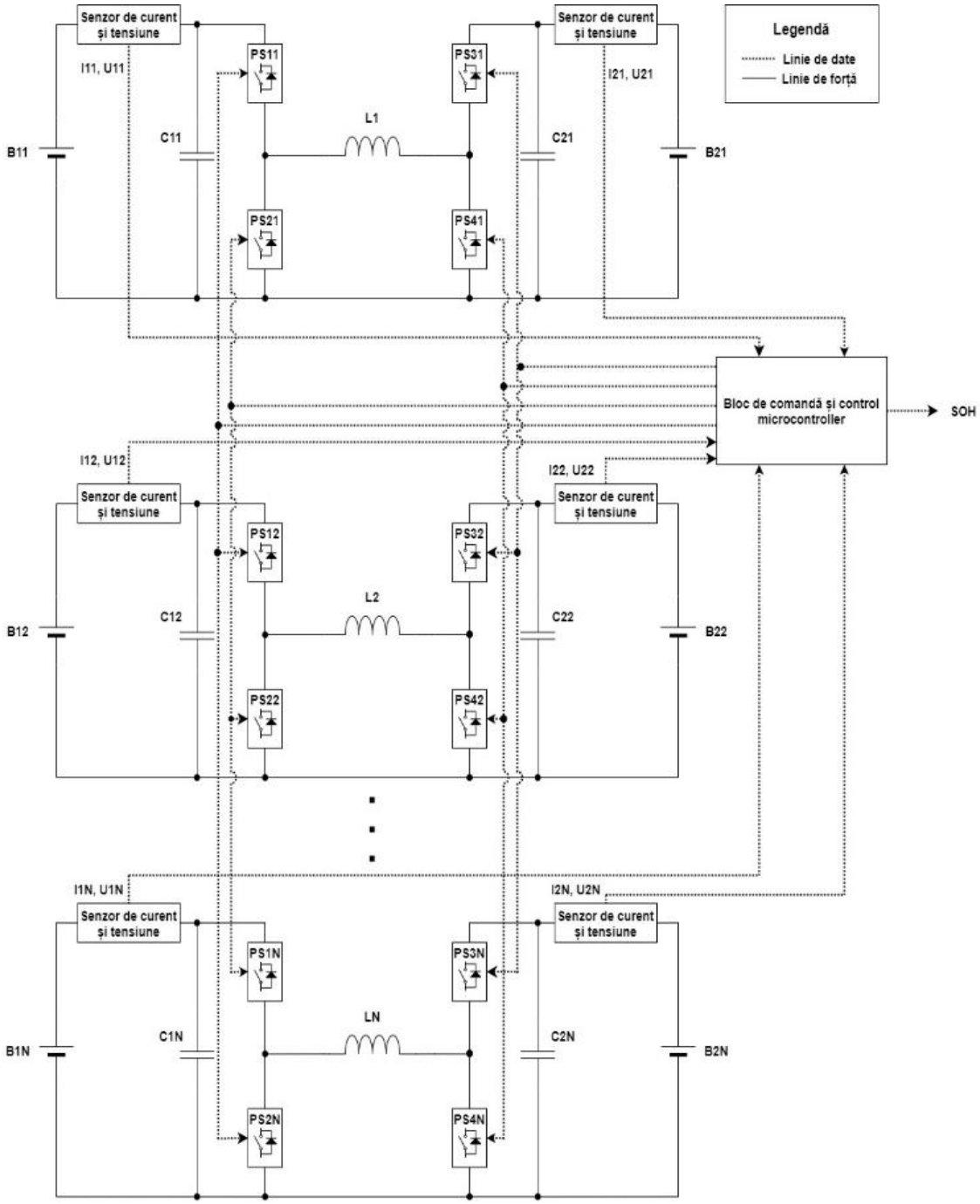

Figura. VII-4. System expansion for 2N batteries.

By implementing these development directions, the proposed system and method will be able to meet future market demands, support technological innovation, and ensure optimal and sustainable battery performance.

BIBLIOGRAPHY

[1] J. Li, S. He, Q. Yang, Z. Wei, Y. Li, and H. He, "A Comprehensive Review of Second Life Batteries Toward Sustainable Mechanisms: Potential, Challenges, and Future Prospects," *IEEE Trans. Transp. Electrification*, vol. 9, no. 4, pp. 4824–4845, Dec. 2023, doi: 10.1109/TTE.2022.3220411.

[2] Q. Dong, S. Liang, J. Li, H. C. Kim, W. Shen, and T. J. Wallington, "Cost, energy, and carbon footprint benefits of second-life electric vehicle battery use," *iScience*, vol. 26, no. 7, p. 107195, Jul. 2023, doi: 10.1016/j.isci.2023.107195.

[3] M. S. H. Lipu *et al.*, "A review of state of health and remaining useful life estimation methods for lithium-ion battery in electric vehicles: Challenges and recommendations," *J. Clean. Prod.*, vol. 205, pp. 115–133, Dec. 2018, doi: 10.1016/j.jclepro.2018.09.065.

[4] J. Sindha, J. Thakur, and M. Khalid, "The economic value of hybrid battery swapping stations with second life of batteries," *Clean. Energy Syst.*, vol. 5, p. 100066, Aug. 2023, doi: 10.1016/j.cles.2023.100066.

[5] Y. Wei and D. Wu, "State of health and remaining useful life prediction of lithium-ion batteries with conditional graph convolutional network," *Expert Syst. Appl.*, vol. 238, p. 122041, Mar. 2024, doi: 10.1016/j.eswa.2023.122041.

[6] Office for Product Safety & Standards, "A Study on the Safety of Second-life Batteries in Battery Energy Storage Systems," Jan. 2023.

[7] C. A. Rufino Júnior *et al.*, "Reviewing Regulations and Standards for Second-Life Batteries," Engineering, preprint, Jun. 2023. doi: 10.20944/preprints202306.0711.v1.

[8] Y. Zhao *et al.*, "A Review on Battery Market Trends, Second-Life Reuse, and Recycling," *Sustain. Chem.*, vol. 2, no. 1, pp. 167–205, Mar. 2021, doi: 10.3390/suschem2010011.

[9] A. A. Kebede *et al.*, "Optimal sizing and lifetime investigation of second life lithium-ion battery for grid-scale stationary application," *J. Energy Storage*, vol. 72, p. 108541, Nov. 2023, doi: 10.1016/j.est.2023.108541.

[10] A. Barré, B. Deguilhem, S. Grolleau, M. Gérard, F. Suard, and D. Riu, "A review on lithium-ion battery ageing mechanisms and estimations for automotive applications," *J. Power Sources*, vol. 241, pp. 680–689, Nov. 2013, doi: 10.1016/j.jpowsour.2013.05.040.

[11] M. Thomas, L. A.-W. Ellingsen, and C. R. Hung, "Research for TRAN Committee - Battery-powered electric vehicles: market development and lifecycle emissions," 2018, doi: 10.2861/038794.

[12] K. Chirumalla, I. Kulkov, V. Parida, E. Dahlquist, G. Johansson, and I. Stefan, "Enabling battery circularity: Unlocking circular business model archetypes and collaboration forms in the electric vehicle battery ecosystem," *Technol. Forecast. Soc. Change*, vol. 199, p. 123044, Feb. 2024, doi: 10.1016/j.techfore.2023.123044.

[13] L. C. Casals, B. Amante García, and C. Canal, "Second life batteries lifespan: Rest of useful life and environmental analysis," *J. Environ. Manage.*, vol. 232, pp. 354–363, Feb. 2019, doi: 10.1016/j.jenvman.2018.11.046.

[14] H. Rallo, G. Benveniste, I. Gestoso, and B. Amante, “Economic analysis of the disassembling activities to the reuse of electric vehicles Li-ion batteries,” *Resour. Conserv. Recycl.*, vol. 159, p. 104785, Aug. 2020, doi: 10.1016/j.resconrec.2020.104785.

[15] J. Zhu *et al.*, “End-of-life or second-life options for retired electric vehicle batteries,” *Cell Rep. Phys. Sci.*, vol. 2, no. 8, p. 100537, Aug. 2021, doi: 10.1016/j.xcrp.2021.100537.

[16] E. Martinez-Laserna *et al.*, “Battery second life: Hype, hope or reality? A critical review of the state of the art,” *Renew. Sustain. Energy Rev.*, vol. 93, pp. 701–718, Oct. 2018, doi: 10.1016/j.rser.2018.04.035.

[17] E. Hossain, D. Murtaugh, J. Mody, H. M. R. Faruque, Md. S. Haque Sunny, and N. Mohammad, “A Comprehensive Review on Second-Life Batteries: Current State, Manufacturing Considerations, Applications, Impacts, Barriers & Potential Solutions, Business Strategies, and Policies,” *IEEE Access*, vol. 7, pp. 73215–73252, 2019, doi: 10.1109/ACCESS.2019.2917859.

[18] J. Urquizo and P. Singh, “A review of health estimation methods for Lithium-ion batteries in Electric Vehicles and their relevance for Battery Energy Storage Systems,” *J. Energy Storage*, vol. 73, p. 109194, Dec. 2023, doi: 10.1016/j.est.2023.109194.

[19] R. R. Kumar, C. Bharatiraja, K. Udhayakumar, S. Devakirubakaran, K. S. Sekar, and L. Mihet-Popa, “Advances in Batteries, Battery Modeling, Battery Management System, Battery Thermal Management, SOC, SOH, and Charge/Discharge Characteristics in EV Applications,” *IEEE Access*, vol. 11, pp. 105761–105809, 2023, doi: 10.1109/ACCESS.2023.3318121.

[20] R. Xiong, L. Li, and J. Tian, “Towards a smarter battery management system: A critical review on battery state of health monitoring methods,” *J. Power Sources*, vol. 405, pp. 18–29, Nov. 2018, doi: 10.1016/j.jpowsour.2018.10.019.

[21] B. Yang *et al.*, “Critical summary and perspectives on state-of-health of lithium-ion battery,” *Renew. Sustain. Energy Rev.*, vol. 190, p. 114077, Feb. 2024, doi: 10.1016/j.rser.2023.114077.

[22] L. Canals Casals, B. Amante García, and L. V. Cremades, “Electric vehicle battery reuse: Preparing for a second life,” *J. Ind. Eng. Manag.*, vol. 10, no. 2, p. 266, May 2017, doi: 10.3926/jiem.2009.

[23] Xiaoyu Li, Tiansi Wang, Lei Pei, Chunbo Zhu, and Bingliang Xu, “A comparative study of sorting methods for Lithium-ion batteries,” in *2014 IEEE Conference and Expo Transportation Electrification Asia-Pacific (ITEC Asia-Pacific)*, Beijing, China: IEEE, Aug. 2014, pp. 1–6. doi: 10.1109/ITEC-AP.2014.6940724.

[24] L. Ungurean, G. Cârstoiu, M. V. Micea, and V. Groza, “Battery state of health estimation: a structured review of models, methods and commercial devices: Battery State of Health Estimation: a Structured Review,” *Int. J. Energy Res.*, vol. 41, no. 2, pp. 151–181, Feb. 2017, doi: 10.1002/er.3598.

[25] E. Kona, “Stationary VRLA battery health estimation by resistance measurement - comparison of dc and ac test methods,” in *2016 IEEE International Conference on Power*

Electronics, Drives and Energy Systems (PEDES), Trivandrum, India: IEEE, Dec. 2016, pp. 1–5. doi: 10.1109/PEDES.2016.7914561.

[26] Y. Li *et al.*, "Data-driven health estimation and lifetime prediction of lithium-ion batteries: A review," *Renew. Sustain. Energy Rev.*, vol. 113, p. 109254, Oct. 2019, doi: 10.1016/j.rser.2019.109254.

[27] B.-A. Enache and E. Diaconescu, "Estimating a battery state of charge using neural networks," in *2014 International Symposium on Fundamentals of Electrical Engineering (ISFEE)*, Bucharest, Romania: IEEE, Nov. 2014, pp. 1–6. doi: 10.1109/ISFEE.2014.7050636.

[28] M. Berecibar, I. Gandiaga, I. Villarreal, N. Omar, J. Van Mierlo, and P. Van Den Bossche, "Critical review of state of health estimation methods of Li-ion batteries for real applications," *Renew. Sustain. Energy Rev.*, vol. 56, pp. 572–587, Apr. 2016, doi: 10.1016/j.rser.2015.11.042.

[29] M. Shahjalal *et al.*, "A review on second-life of Li-ion batteries: prospects, challenges, and issues," *Energy*, vol. 241, p. 122881, Feb. 2022, doi: 10.1016/j.energy.2021.122881.

[30] A. Farmann, W. Waag, A. Marongiu, and D. U. Sauer, "Critical review of on-board capacity estimation techniques for lithium-ion batteries in electric and hybrid electric vehicles," *J. Power Sources*, vol. 281, pp. 114–130, May 2015, doi: 10.1016/j.jpowsour.2015.01.129.

[31] B.-A. Enache, G.-C. Seritan, and C. Cepisca, "Comparative study of screening methods for second-life LiFePO4 batteries," *Rev Roum Sci Techn– Électrotechn Énerg*, vol. 65, no. 1–2, pp. 71–74, 2020.

[32] S. Yang, C. Zhang, J. Jiang, W. Zhang, L. Zhang, and Y. Wang, "Review on state-of-health of lithium-ion batteries: Characterizations, estimations and applications," *J. Clean. Prod.*, vol. 314, p. 128015, Sep. 2021, doi: 10.1016/j.jclepro.2021.128015.

[33] Y. Guo, K. Huang, and X. Hu, "A state-of-health estimation method of lithium-ion batteries based on multi-feature extracted from constant current charging curve," *J. Energy Storage*, vol. 36, p. 102372, Apr. 2021, doi: 10.1016/j.est.2021.102372.

[34] J. He, S. Meng, X. Li, and F. Yan, "Partial Charging-Based Health Feature Extraction and State of Health Estimation of Lithium-Ion Batteries," *IEEE J. Emerg. Sel. Top. Power Electron.*, vol. 11, no. 1, pp. 166–174, Feb. 2023, doi: 10.1109/JESTPE.2022.3143831.

[35] C. Lin, J. Xu, M. Shi, and X. Mei, "Constant current charging time based fast state-of-health estimation for lithium-ion batteries," *Energy*, vol. 247, p. 123556, May 2022, doi: 10.1016/j.energy.2022.123556.

[36] S. K. Pradhan and B. Chakraborty, "Battery management strategies: An essential review for battery state of health monitoring techniques," *J. Energy Storage*, vol. 51, p. 104427, Jul. 2022, doi: 10.1016/j.est.2022.104427.

[37] M. M. Camboim *et al.*, "State of health estimation of second-life batteries through electrochemical impedance spectroscopy and dimensionality reduction," *J. Energy Storage*, vol. 78, p. 110063, Feb. 2024, doi: 10.1016/j.est.2023.110063.

[38] S. Zhang, X. Guo, X. Dou, and X. Zhang, “A rapid online calculation method for state of health of lithium-ion battery based on coulomb counting method and differential voltage analysis,” *J. Power Sources*, vol. 479, p. 228740, Dec. 2020, doi: 10.1016/j.jpowsour.2020.228740.

[39] R. Zhou, R. Zhu, C.-G. Huang, and W. Peng, “State of health estimation for fast-charging lithium-ion battery based on incremental capacity analysis,” *J. Energy Storage*, vol. 51, p. 104560, Jul. 2022, doi: 10.1016/j.est.2022.104560.

[40] X. Feng *et al.*, “Online State-of-Health Estimation for Li-Ion Battery Using Partial Charging Segment Based on Support Vector Machine,” *IEEE Trans. Veh. Technol.*, vol. 68, no. 9, pp. 8583–8592, Sep. 2019, doi: 10.1109/TVT.2019.2927120.

[41] T. Sun, R. Wu, Y. Cui, and Y. Zheng, “Sequent extended Kalman filter capacity estimation method for lithium-ion batteries based on discrete battery aging model and support vector machine,” *J. Energy Storage*, vol. 39, p. 102594, Jul. 2021, doi: 10.1016/j.est.2021.102594.

[42] J. Jia, J. Liang, Y. Shi, J. Wen, X. Pang, and J. Zeng, “SOH and RUL Prediction of Lithium-Ion Batteries Based on Gaussian Process Regression with Indirect Health Indicators,” *Energies*, vol. 13, no. 2, p. 375, Jan. 2020, doi: 10.3390/en13020375.

[43] S. B. Sarmah *et al.*, “A Review of State of Health Estimation of Energy Storage Systems: Challenges and Possible Solutions for Futuristic Applications of Li-Ion Battery Packs in Electric Vehicles,” *J. Electrochem. Energy Convers. Storage*, vol. 16, no. 4, p. 040801, Nov. 2019, doi: 10.1115/1.4042987.

[44] J. Tian, R. Xiong, and W. Shen, “A review on state of health estimation for lithium ion batteries in photovoltaic systems,” *eTransportation*, vol. 2, p. 100028, Nov. 2019, doi: 10.1016/j.etran.2019.100028.

[45] Z. Wang, X. Zhao, L. Fu, D. Zhen, F. Gu, and A. D. Ball, “A review on rapid state of health estimation of lithium-ion batteries in electric vehicles,” *Sustain. Energy Technol. Assess.*, vol. 60, p. 103457, Dec. 2023, doi: 10.1016/j.seta.2023.103457.

[46] F. Von Bülow, J. Mentz, and T. Meisen, “State of health forecasting of Lithium-ion batteries applicable in real-world operational conditions,” *J. Energy Storage*, vol. 44, p. 103439, Dec. 2021, doi: 10.1016/j.est.2021.103439.

[47] D. Pan, H. Li, and Y. Song, “A Comparative Study of Particle Filters and its Variants in Lithium-ion Battery SOH Estimation,” in *2020 International Conference on Sensing, Measurement & Data Analytics in the era of Artificial Intelligence (ICSMD)*, Xi’an, China: IEEE, Oct. 2020, pp. 198–203. doi: 10.1109/ICSMD50554.2020.9261654.

[48] F. Zhu and J. Fu, “A Novel State-of-Health Estimation for Lithium-Ion Battery via Unscented Kalman Filter and Improved Unscented Particle Filter,” *IEEE Sens. J.*, vol. 21, no. 22, pp. 25449–25456, Nov. 2021, doi: 10.1109/JSEN.2021.3102990.

[49] F. von Bülow and T. Meisen, “A review on methods for state of health forecasting of lithium-ion batteries applicable in real-world operational conditions,” *J. Energy Storage*, vol. 57, p. 105978, Jan. 2023, doi: 10.1016/j.est.2022.105978.

[50] S. Li, Z. Fu, J. Zhu, and Y. Yuan, “Estimation of State-of-Health for Lithium-Ion Battery Based on Increment Capacity Analysis Method and Long Short-Term Memory Neural Network,” in *2023 IEEE/IAS Industrial and Commercial Power System Asia (I&CPS Asia)*, Chongqing, China: IEEE, Jul. 2023, pp. 1818–1823. doi: 10.1109/ICPSAsia58343.2023.10294949.

[51] M. Şahin, “A comprehensive analysis of weighting and multicriteria methods in the context of sustainable energy,” *Int. J. Environ. Sci. Technol.*, vol. 18, no. 6, pp. 1591–1616, Jun. 2021, doi: 10.1007/s13762-020-02922-7.

[52] *** Jon P. Christopherson, “USABC Battery Test Manual For Electric Vehicles Rev. 3.” Jun. 2015. [Online]. Available: chrome-extension://efaidnbmnnnibpcajpcglclefindmkaj/https://inldigitallibrary.inl.gov/sites/sti/sti/6492291.pdf

[53] M. Arrinda *et al.*, “Application Dependent End-of-Life Threshold Definition Methodology for Batteries in Electric Vehicles,” *Batteries*, vol. 7, no. 1, p. 12, Feb. 2021, doi: 10.3390/batteries7010012.

[54] Z. Yu, B. Lv, R. Huai, L. Chang, Z. Sun, and H. Li, “Research on rapid extraction of internal resistance of lithium battery based on short-time transient response,” *J. Energy Storage*, vol. 77, p. 109985, Jan. 2024, doi: 10.1016/j.est.2023.109985.

[55] E. Braco, I. San Martín, P. Sanchis, and A. Ursúa, “Fast capacity and internal resistance estimation method for second-life batteries from electric vehicles,” *Appl. Energy*, vol. 329, p. 120235, Jan. 2023, doi: 10.1016/j.apenergy.2022.120235.

[56] Y. Wang, S.-Y. Kim, Y. Chen, H. Zhang, and S.-J. Park, “An SMPS-Based Lithium-Ion Battery Test System for Internal Resistance Measurement,” *IEEE Trans. Transp. Electrification*, vol. 9, no. 1, pp. 934–944, Mar. 2023, doi: 10.1109/TTE.2022.3178981.

[57] A. Tang, P. Gong, Y. Huang, X. Wu, and Q. Yu, “Research on pulse charging current of lithium-ion batteries for electric vehicles in low-temperature environment,” *Energy Rep.*, vol. 9, pp. 1447–1457, Sep. 2023, doi: 10.1016/j.egyr.2023.04.226.

[58] L. Wang, X. Zhao, Z. Deng, and L. Yang, “Application of electrochemical impedance spectroscopy in battery management system: State of charge estimation for aging batteries,” *J. Energy Storage*, vol. 57, p. 106275, Jan. 2023, doi: 10.1016/j.est.2022.106275.

[59] S. Barcellona, S. Colnago, and L. Piegari, “Analysis of the lithium-ion batteries resistance hysteresis phenomenon,” in *2022 International Symposium on Power Electronics, Electrical Drives, Automation and Motion (SPEEDAM)*, Sorrento, Italy: IEEE, Jun. 2022, pp. 46–51. doi: 10.1109/SPEEDAM53979.2022.9842069.

[60] M. A. Hoque *et al.*, “Data driven analysis of lithium-ion battery internal resistance towards reliable state of health prediction,” *J. Power Sources*, vol. 513, p. 230519, Nov. 2021, doi: 10.1016/j.jpowsour.2021.230519.

[61] A. Blidberg, “Correlation between different impedance measurement methods for battery cells,” *KTH Chem. Sci. Eng.*, 2012.

[62] G. Piłatowicz, A. Marongiu, J. Drillkens, P. Sinhuber, and D. U. Sauer, "A critical overview of definitions and determination techniques of the internal resistance using lithium-ion, lead-acid, nickel metal-hydride batteries and electrochemical double-layer capacitors as examples," *J. Power Sources*, vol. 296, pp. 365–376, Nov. 2015, doi: 10.1016/j.jpowsour.2015.07.073.

[63] L. Pei, T. Wang, R. Lu, and C. Zhu, "Development of a voltage relaxation model for rapid open-circuit voltage prediction in lithium-ion batteries," *J. Power Sources*, vol. 253, pp. 412–418, May 2014, doi: 10.1016/j.jpowsour.2013.12.083.

[64] M.-Y. Zhou, J.-B. Zhang, C.-J. Ko, and K.-C. Chen, "Precise prediction of open circuit voltage of lithium ion batteries in a short time period," *J. Power Sources*, vol. 553, p. 232295, Jan. 2023, doi: 10.1016/j.jpowsour.2022.232295.

[65] Y. Muratoglu and A. Alkaya, "Unscented Kalman Filter based State of Charge Estimation for the Equalization of Lithium-ion Batteries on Electrical Vehicles," *Eng. Technol. Appl. Sci. Res.*, vol. 9, no. 6, pp. 4876–4882, Dec. 2019, doi: 10.48084/etasr.3111.

[66] D. Theuerkauf and L. Swan, "Characteristics of Open Circuit Voltage Relaxation in Lithium-Ion Batteries for the Purpose of State of Charge and State of Health Analysis," *Batteries*, vol. 8, no. 8, p. 77, Jul. 2022, doi: 10.3390/batteries8080077.

[67] T.-I. Voicilă, G.-C. Seriţan, B.-A. Enache, R. Porumb, and M. Stănculescu, "First Steps Towards the Design of a multi-Chemistry, multi-Battery State of Health Screening System," in *2023 13th International Symposium on Advanced Topics in Electrical Engineering (ATEE)*, IEEE, 2023, pp. 1–6.

[68] PhD Student., Doctoral School of Electrical Engineering, University POLITEHNICA of Bucharest, S. Gkanatsios, I. Vilciu, Lecturer, Department of Measurements, Electrical Apparatus and Static Converters, University POLITEHNICA of Bucharest, T.-I. Voicila, and Professor Assistant, Department of Measurements, Electrical Apparatus and Static Converters, University POLITEHNICA of Bucharest, "Evaluating the state of health of lead-acid battery used in UPS," *EMERG - Energy Environ. Effic. Resour. Glob.*, vol. 9, no. 3, pp. 50–61, 2023, doi: 10.37410/EMERG.2023.3.03.

[69] D. Zhan, "White Paper - Design Considerations for a Bidirectional DC/DC Converter," *Ind. Analog Power Group Renesas Electron. Corp*, Sep. 2018, Accessed: Oct. 13, 2023. [Online]. Available: https://www.renesas.com/us/en/document/whp/design-considerations-bidirectional-dcdc-converter

[70] Ping-Ching Huang, Wei-Quan Wu, Hsin-Hsin Ho, and Ke-Horng Chen, "Hybrid Buck–Boost Feedforward and Reduced Average Inductor Current Techniques in Fast Line Transient and High-Efficiency Buck–Boost Converter," *IEEE Trans. Power Electron.*, vol. 25, no. 3, pp. 719–730, Mar. 2010, doi: 10.1109/TPEL.2009.2031803.

[71] Z. Zhou, H. Li, and X. Wu, "A Constant Frequency ZVS Control System for the Four-Switch Buck–Boost DC–DC Converter With Reduced Inductor Current," *IEEE Trans. Power Electron.*, vol. 34, no. 7, pp. 5996–6003, Jul. 2019, doi: 10.1109/TPEL.2018.2884950.

[72] TI Designs: SLVA535B, “Basic Calculations of a 4 Switch Buck-Boost Power Stage.” Accessed: May 17, 2023. [Online]. Available: https://www.ti.com/lit/an/slva535b/slva535b.pdf?ts=1684332497303&ref_url=https%253A%252F%252Fwww.google.com%252F

[73] TI Designs: SLVA372D, “Basic Calculation of a Boost Converter’s Power Stage.” Accessed: May 17, 2023. [Online]. Available: https://www.ti.com/lit/an/slva372d/slva372d.pdf?ts=1684302905583&ref_url=https%253A%252F%252Fwww.google.com%252F

[74] TI Application Report: SLVA477B, “Basic Calculation of a Buck Converter’s Power Stage.” Accessed: May 17, 2023. [Online]. Available: https://www.ti.com/lit/an/slva477b/slva477b.pdf?ts=1684301546101&ref_url=https%253A%252F%252Fwww.google.com%252F

[75] *** Wurth Elektronik, “Datasheet WE-HCF Round Wire SMT High Current Inductor, 74437529203221.” Apr. 26, 2023. [Online]. Available: chrome-extension://efaidnbmnnnibpcajpcglclefindmkaj/https://www.we-online.com/components/products/datasheet/74437529203221.pdf

[76] *** Wurth Elektronik, “Datasheet WCAP-PSHP Aluminum Polymer Capacitors, 875115655003.” Jun. 02, 2023. [Online]. Available: chrome-extension://efaidnbmnnnibpcajpcglclefindmkaj/https://www.we-online.com/components/products/datasheet/875115655003.pdf

[77] ***, “Datasheet IRF530NSPbF.” [Online]. Available: chrome-extension://efaidnbmnnnibpcajpcglclefindmkaj/https://www.infineon.com/dgdl/irf530nspbf.pdf?fileId=5546d462533600a4015355e38eb4199c

[78] *** Linear Technology Corp., “Datasheet High Voltage Synchronous N-Channel MOSFET Driver, LTC4444-5”, [Online]. Available: chrome-extension://efaidnbmnnnibpcajpcglclefindmkaj/https://www.analog.com/media/en/technical-documentation/data-sheets/4449fa.pdf

[79] *** Kemet, “Datasheet Tantalum Surface Mount Capacitors, T499A224K035ATE18K.” Dec. 07, 2023. [Online]. Available: chrome-extension://efaidnbmnnnibpcajpcglclefindmkaj/https://connect.kemet.com:7667/gateway/IntelliData-ComponentDocumentation/1.0/download/datasheet/T499A224K035ATE18K

[80] *** ROHM, “Datasheet Schottky Barrier Diode, RB075BGE40S.” Dec. 07, 2019. [Online]. Available: https://www.rohm.com/datasheet?p=RB075BGE40S&dist=Digi-key&media=referral&source=digi-key.com&campaign=Digi-key

[81] N. Campagna *et al.*, “Battery models for battery powered applications: A comparative study,” *Energies*, vol. 13, no. 16, p. 4085, 2020.

[82] T.-I. Voicila, G.-C. Seritan, B.-A. Enache, M. Stanculescu, and R.-F. Porumb, “Design and implementation of a multi-battery, multi-chemistry state of health screening system,” in *2023 10th International Conference on Modern Power Systems (MPS)*, Cluj-Napoca, Romania: IEEE, Jun. 2023, pp. 1–4. doi: 10.1109/MPS58874.2023.10187442.

[83] C. H. Gandescu, S. Gkanatsios, C. Cepisca, I. Vilciu, and T.-I. Voicila, “Accurate Modelling of an Online Uninterrupted Power Supply”.

[84] *** S. Espressif, “Esp32 datasheet,” *IotY Based Microcontroller*, 2017.

[85] *** Adafruit Industries LLC, “Datasheet INA219 High Side DC Current Sensor Breakout - 26V +/- 3.2A Max, ID 904.” [Online]. Available: chrome-extension://efaidnbmnnnibpcajpcglclefindmkaj/https://mm.digikey.com/Volume0/opasdata/d220001/medias/docus/1860/904_Web.pdf

[86] *** Adafruit, “Datasheet Shield-LCD16x2.” [Online]. Available: chrome-extension://efaidnbmnnnibpcajpcglclefindmkaj/https://www.tme.eu/Document/8a4fa5818a91f3c03fe1ef0e62962b73/SHIELD-LCD16x2.pdf

[87] J. Yu, B. Mo, D. Tang, J. Yang, J. Wan, and J. Liu, “Indirect State-of-Health Estimation for Lithium-Ion Batteries under Randomized Use,” *Energies*, vol. 10, no. 12, p. 2012, Dec. 2017, doi: 10.3390/en10122012.

[88] P. Venugopal and V. T., “State-of-Health Estimation of Li-ion Batteries in Electric Vehicle Using IndRNN under Variable Load Condition,” *Energies*, vol. 12, no. 22, p. 4338, Nov. 2019, doi: 10.3390/en12224338.